SIMULATION AND OPTIMIZATION OF A WATER-GAS SHIFT REACTOR

A Thesis Submitted
In Partial Fulfilment of the Requirements
for the Degree of
MASTER OF TECHNOLOGY

By
K. K. PAHUJA

to the

DEPARTMENT OF CHEMICAL ENGINEERING
INDIAN INSTITUTE OF TECHNOLOGY KANPUR
APRIL 1973

TO

MY PARENTS

CERTIFICATE

It is to certify that this work "Simulation and Optimization of a Water-Gas Shift Reactor" has been carried out under my supervision and that this work has not been submitted elsewhere for a degree.

Dated: April 30, 1973

D.N. Saraf
Assistant Professor
Department of Chemical Engineering
Indian Institute of Technology, Kanpur

ACKNOWLEDGEMENTS

The author is deeply indebted to Dr. D.N. Saraf for his valuable guidance and kind encouragement during the course of this investigation. The valuable suggestions given by Dr. S.C. Mehta are also gratefully acknowledged.

Thanks are due to the Computer Centre of I.I.T./Kanpur for providing sufficient computer time for the work.

The author is also thankful to Mr. B.S. Pandey for typing the manuscript.

Author

CONTENTS

LIST OF FIGURES

***

LIST OF TABLES

...

NOMENCLATURE

A_f	Ageing factor
$(C_p)_i$	Molal heat capacity of component, i, cal/(mole)(°K)
D_{eff}	Effective diffusivity in catalyst pores, $cm^2/sec.$
D_P	Equivalent diameter of catalyst pellet, cm.
E	Effectiveness factor
e	Voidage of catalyst bed
E_a	Intrinsic activation energy, cal/mole
F	Total flow of gas mixture, $NM^3/hr.$
f	Fugacity of pure component
F_a	Constant used for defining pressure dependency of rate constant, atm.
f_s	Sulfur factor
ΔH_R	Heat of reaction, cal/mole of CO
(H_2S)	Concentration of H_2S (dry basis), ppm.
k, k', k_2, k_2', k_1	Reaction rate constants, dimensions defined by their respective equations
ka_1	Apparent (pseudo) first-order reaction rate constant, $(NM^3$ of gas$)/(M^3$ catalyst bed$)$(hr)
ko_1	Apparent (pseudo) first-order reaction rate constant, $(M^3$ gas at P and T$)/(M^3$ catalyst bed$)$(sec.)
kv_1	Intrinsic (pseudo) first order reaction rate constant, $(M^3$ gas at P and T$)/(M^3$ catalyst particles$)$(Sec)
K	Equilibrium constant for water-gas shift reaction
K'	Equilibrium constant for the reverse shift reaction, $=1/K$
K_{CO}, K_{CO_2} etc.	Adsorption equilibrium constants for the components CO, CO_2 etc. in the rate equation
m	Thiele modulus

P	Total pressure, atm.
p_i	Partial pressure of component i
R	Gas constant = 1.987 cal/(mole)(°K)
r	Rate of reaction, $\frac{NM^3 \text{ of CO converted}}{(M^3 \text{ bed volume})(hr)}$
T	Temperature, °K
t	time, days
V	Volume of reactor bed, M^3
x	Degree of conversion
y_i	Mole fraction of component i
$y_{f,i}$	Mole fraction of component i in feed stream
Z_1	Preexponential factor of intrinsic rate constant, sec^{-1}

NOTE: * has been used as a multiplication symbol at some places

Subscripts

n	Bed-number
$n,0$	Inlet of bed n
n,L	exit of bed n

Superscripts

$*$	Equilibrium conditions

"SIMULATION AND OPTIMIZATION OF A WATER-GAS SHIFT REACTOR"

by

K.K. PAHUJA

Department of Chemical Engineering
Indian Institute of Technology, Kanpur

ABSTRACT

A simulation model for the water-gas shift reactor is developed using the kinetic data for the FCI H.T. shift catalyst to estimate the values of the reaction rate constant The model takes into account the effect of diffusion within the catalyst pores. The model appears capable of supplying results in reasonable agreement with the plant measurements.

The model is used next to prepare an optimization scheme for optimizing an existing industrial reactor with maximum CO-conversion as the criterion. The computations have been made on IBM 7044 computer. An improvement in the plant conversion from 87.97% to 91.14% is predicted at the given feed composition and the reactor load. The effect of the various parameters like steam/gas ratio, dry gas feed rate and catalyst age on the optimum conversion is also studie Over the range studied, the optimum CO-conversion increases with increasing steam/gas ratio, decreases linearly with increasing dry gas feed rate and is hardly affected by cataly ageing beyond a period of 270 days.

***

CHAPTER 1

INTRODUCTION

The recent trend in the study of process systems is through simulation. Simulation can be broadly defined as representing a physical process or phenomenon by means of a mathematical model.

Off-line computer simulation of an actual plant can provide a priori knowledge of the behaviour of the plant, provided that the mathematical model chosen for simulation describes the plant with reasonable accuracy. The simulation model achieved by writing down the process equations based on the physical and chemical operations involved in the plant is programmed on a relatively large off-line digital computer and experiments are performed on the simulated plant to observe the effect of changing independent variables on the plant performance. This type of computer simulation is faster and cheapter than experimentation on a running plant. In addition, the range of independent variables for simulation can be larger than that observed normally in a plant in a day-to-day operation.

In the present work, a simulation study on an industrial shift reactor has been carried out with the purpose of using the simulation model in conjunction with an optimization scheme for determining the key variables that will yield maximum conversion.

Description of the Reactor:

The industrial reactor concerned in the present work is the multi-bed CO converter of the Fertilizer Corporation of India, Trombay. The reactor is shown schematically in Fig. 1.1. In the preparation of ammonia synthesis gas, after partial oxidation of Naphtha, the product gas contains hydrogen and carbon monoxide as the major components. In the converter, this carbon monoxide is converted with steam to produce additional hydrogen via the shift reaction

$$CO + H_2O(g) \rightleftharpoons CO_2 + H_2.$$

The reaction is carried out in the temperature range of 330-500°C in the presence of Chromia promoted iron-oxide catalyst (high temperature shift catalyst) developed by Fertilizer Corporation of India - Planning and Development Division.

Before entering the converter, the gas is saturated with water in a heater-saturator, mixed with steam and is further heated in a preheater. The converter consists of three catalyst beds, which are essentially adiabatic. Usually the first stage is operated at a higher temperature to get fast rate of reaction, and the last stage is operated at a lower temperature to increase the equilibrium conversion of CO. For removing the exothermic heat of reaction, the gas between the beds is cooled in interstage coolers.

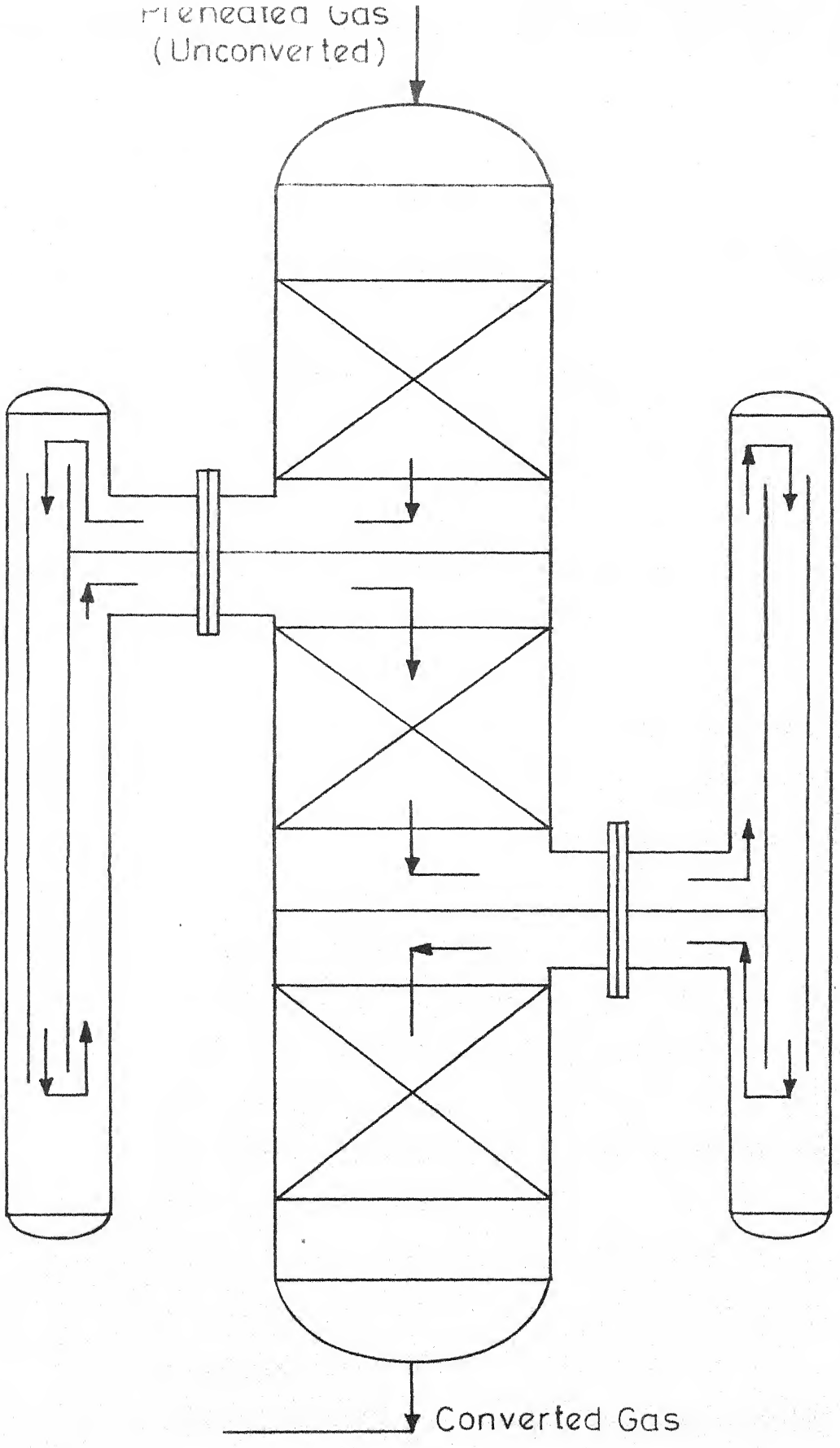

Fig.1.1 - Schematic Diagram of CO-Converter.

CHAPTER 2

THEORY

I. Steps in Gas-Solid Catalytic Reactions:

The major role played by the catalyst in a reaction is that it increases the rate of reaction because it makes possible an alternative mechanism, each step of which has a lower free energy of activation than that for the uncatalyzed process, without affecting the state of equilibrium between the products and reactants.

In a gaseous reaction within a packed-bed catalytic reactor, the various physical and chemical processes have to be taken into account while considering the overall catalytic process. The different steps involved are:

1. Mass-transfer of reactants from the fluid phase to the external surface of the catalyst particles.
2. Diffusion of reactants into the pores of the catalyst particles.
3. Adsorption of reactants on the catalyst surface.
4. Reaction on the surface.
5. Desorption of products from the catalyst particles.
6. Diffusion of products out from the pores of the catalyst particles.
7. Mass-transfer of products from the external surface into the fluid phase.

The steps 1, 2, 6, and 7 are entirely of a physical nature, whereas the steps 3, 4 and 5 are chemical phenomenon.

External Diffusion:

The rate of diffusion, r_D, can be expressed by the relation

$$r_D = k_g \, a \, (p_g - p_i) \qquad (2.1)$$

Where

p_g = partial pressure of diffusing gas in bulk stream

p_i = partial pressure of diffusing gas at solid surface

k_g = diffusion rate constant or coefficient

a = external area of catalyst particle per unit mass.

The diffusion-rate constant depends upon the nature of the diffusing component, turbulence conditions in the vicinity of the catalyst particle and properties of the entire gas mixture The effect of bulk diffusion is the most important when rate of reaction is high and linear gas velocity is low. In fixed-bed reactors, where the fluid velocity is high with respect to the solid, molecular diffusion will play a small role in determining the rate of mass transfer.

III. Internal Diffusion in Porous Catalysts:

Highly active catalyst pellets obtained by compressing finely divided powder, are porous and usually possess a large amount of internal surface. It is necessary for the reagents

to succeed in reacting this internal surface, and this will involve diffusion within the pores.

The measured rate of reaction on a porous catalyst includes the resistance of internal diffusion. The factors which increase the importance of diffusion are an active catalyst surface, a high temperature, a large particle size, and small pore diameter. When the diffusion resistance is significant, the activation energy, form of the rate equation (order of reaction), and other kinetic factors become dependent upon pore size and particle size. The internal diffusion results in an apparent decrease of the energy of activation with increasing temperature.

Two kinds of diffusion in pores are possible. If the pores are large and the gas density is high, the process is that of bulk, or ordinary diffusion. The effective diffusion coefficient, D_{eff}, will be given by

$$D_{eff} = D\varepsilon / \tau \qquad (2.2)$$

Where D is the ordinary diffusion coefficient, ε is the voidage and τ is the tortuosity factor which has to be introduced due to the pores being neither straight nor of uniform cross-section. The diffusivity is inversely proportional to the pressure.

If the pores are quite small, and/or the gas density is low, the molecules collide with the pore wall much more

frequently than with each other. This is known as 'Knudsen diffusion'. The Knudsen diffusion coefficient for a straight round pore is given by

$$D_k = 9700\, r_e \sqrt{T/M} \qquad Cm^2/Sec \qquad (2.3)$$

Where

r_e = equivalent radius of pore, cm.

T = Temperature, °K

M = Molecular weight of the component.

Pressure has no effect on this diffusivity.

IV. Catalyst Effectiveness:

Since diffusion requires a concentration gradient, the concentration of reactants will be less in the centre of a catalyst particle than at its outer surface. Hence the reaction rate will in general be less at the centre than at the outside surface.

A quantitative evaluation of the influence of pore diffusion on the rate of reaction can be performed by introducing the term 'effectiveness factor', E. This is defined as the ratio of the observed rate to that which would be obtained if the whole of the internal surface of the pellet were available to the reagents at the same concentration as they have at the external surface.

The mathematical analysis for determining the effectiveness of a porous catalyst in case of simultaneous diffusion and reaction becomes simplified by considering a spherical catalyst pellet and assuming isothermal conditions. It is further assumed that the complicated diffusion phenomenon within the porous structure can be represented by a single overall effective diffusion coefficient, D_{eff}.

For a reaction in which there is no change in number of moles on reaction, a steady state mass balance on a differential spherical shell of radius R_p and thickness dR_p gives

$$\frac{d^2C}{d R_p^2} + \frac{2}{R_p} \frac{dC}{dR_p} = \frac{r}{D_{eff}} \qquad (2.4)$$

Where r = reaction rate per unit volume of catalyst pellet.

C = concentration of reagent.

The above equation is to be solved for the boundary conditions:

i) $C = C_S$ at $R_p = R_S$

(i.e. the outside surface of the pellet).

ii) $\frac{dC}{dR_p} = 0$ at $R_p = 0$

(i.e. no concentration gradient will exist at the centre of the sphere).

Solution of the differential eqn.(2.4) subject to the given boundary conditions describes the concentration profile in the catalyst pellet. For reactions of other than first order, analytical solution of this equation becomes more difficult.

V. The Optimization of Exothermic Equilibrium Reactions:

The optimization of the reactor output - i.e. maximization of the amount of reaction product per unit of time and reactor volume may play an important part in case of reversible exothermic reactions[1]. For such reactions the effect of a temperature increase is to raise the speed of the forward reaction but also to lower the value of the equilibrium constant and thereby to reduce the maximum attainable conversion. Thus the kinetic and thermodynamic factors are, in a certain sense, in opposition. A compromise must then be found between the requirements of a high degree of conversion (low temperature) and those of a high average reaction rate. Near the inlet to the tubular reactor, where the reacting gas is still far from equilibrium, it is advantageous to use a fairly high temperature in order to increase the forward reaction rate and thereby to raise the reactor output. Near the outlet to the reactor, however, the temperature should be brought to a much lower level so that a better equilibrium state may be approached.

For a reversible exothermic reaction, the rate will pass through a maximum as a function of temperature when the composition of the reaction mixture is constant (Fig. 2.1).

At a low temperature, the reaction rate, r, will be small, whereas a high temperature, T*, will exist at which the mixture is in equilibrium and the rate is zero. The temperature

at which the rate is a maximum will be somewhat lower than T* and is determined by the condition

$$\frac{\partial r}{\partial T} = 0 \qquad (2.5)$$

The optimum temperature profile in a tubular reactor can be found on the assumption that the criterion (2.5) must be valid for any cross section of the reactor. Then the reaction rate has its maximum value as a function of temperature at any degree of conversion. However in practice, the establishment of the optimum temperature profile to maximize the reactor output, involves technical difficulties and expensive provisions because of the very special schedule of heat removal which would be required. For gas reactions in a catalytic reactor, it is much simpler from a technical point of view, to let the reaction proceed adiabatically. A reasonably close approximation to the maximum rate path can then be achieved by carrying out the reaction in a multistage tubular reactor with interstage cooling of the reaction mixture by means of heat exchangers (Ref. Fig. 2.2).

Each catalyst section operates adiabatically and consequently the temperature rises from inlet to outlet which, of course, is contrary to the theoretical ideal. However, by removing heat from the gas after it leaves each section, the temperature is brought to a much lower level at the entrance to the next section in the series. Thus an approximation to

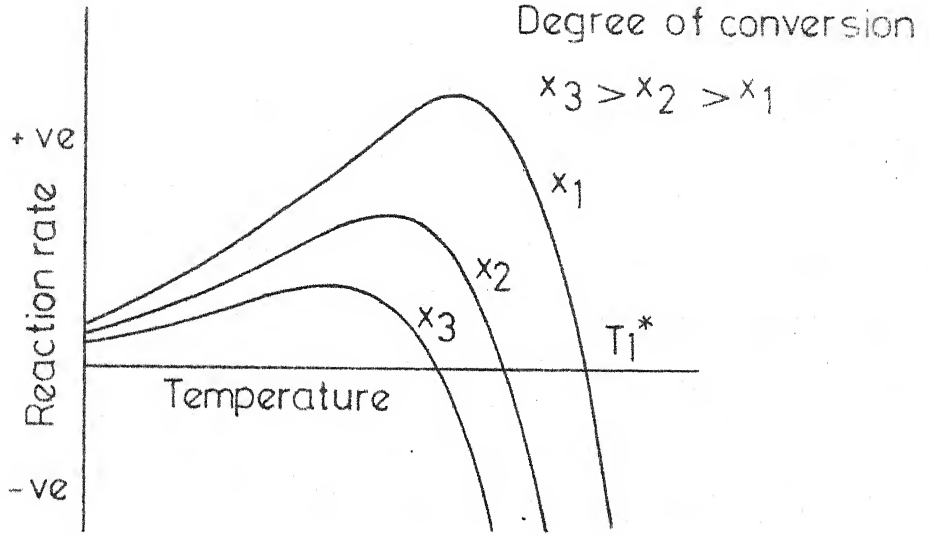

Fig. 2·1 - Reaction rate as a function of Temperature.

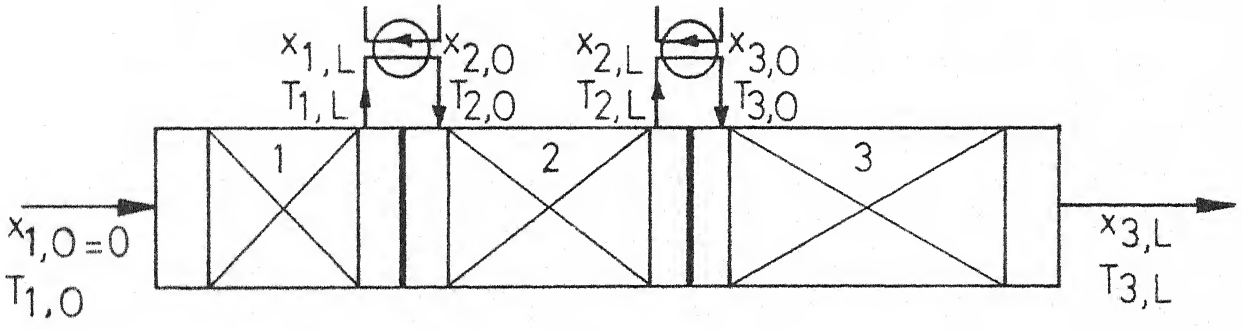

Fig. 2·2 - Multi-stage adiabatic tubular reactor with cooling between sections.

the optimum sequence is obtained by stepwise change. HORN and KUCHLER[2] provided the solution to the problem of optimizing such a system, i.e. that of determining the highest possible final conversion for a given number of sections and for a given entrance temperature of the first section. (This is equivalent to determining the temperature sequence which will result in a minimum quantity of catalyst for the attainment of some chosen hourly output of product[3]). The inlet temperature of the first stage, $T_{1,0}$, is an independent parameter which has to be varied in order to find the minimum amount of catalyst needed for a certain final degree of conversion, or the maximum degree of conversion obtainable with a given amount of catalyst in a given number of sections. For an N-bed sequence (Fig.2.2) the conditions for this optimization as given by Kramer[4] are (Ref. Appendix I):

i) For the optimum temperature policy, the condition for each section (index n) is:

$$\int_{x_{n,0}}^{x_{n,L}} \frac{1}{r^2} \cdot \frac{\partial r}{\partial T} \cdot dx = 0 \qquad n = 1,2,\ldots,N \qquad (2.6)$$

Where, x = relative degree of conversion

The above integral is to be evaluated along adiabatic paths.

ii) Between two sections (n-1) and n:

$$r_{(n-1),L} = r_{n,0} \qquad n = 2,3,.....,N \tag{2.7}$$

This condition relates $T_{n,0}$ to $T_{(n-1),L}$ since for the inter-stage coolers it is clear that

$$x_{(n-1),L} = x_{n,0} \tag{2.7a}$$

and

$$T_{n,0} < T_{(n-1),L}. \tag{2.7b}$$

The criteria represented by equation (2.7) implies that the rate of reaction at the exit of a bed should be the same as that at the inlet to the next. This is possible because of the double valued nature of the rate function (Ref.Fig.2.1).

It may occur that $T_{1,L}$ exceeds the maximum permissible temperature, T_m, so that only a corresponding degree of conversion x_m ($< x_{1,L}$) can be reached in the first section. In that case, eqn.(2.7) will not apply any more for finding the proper entrance temperature to the second section.

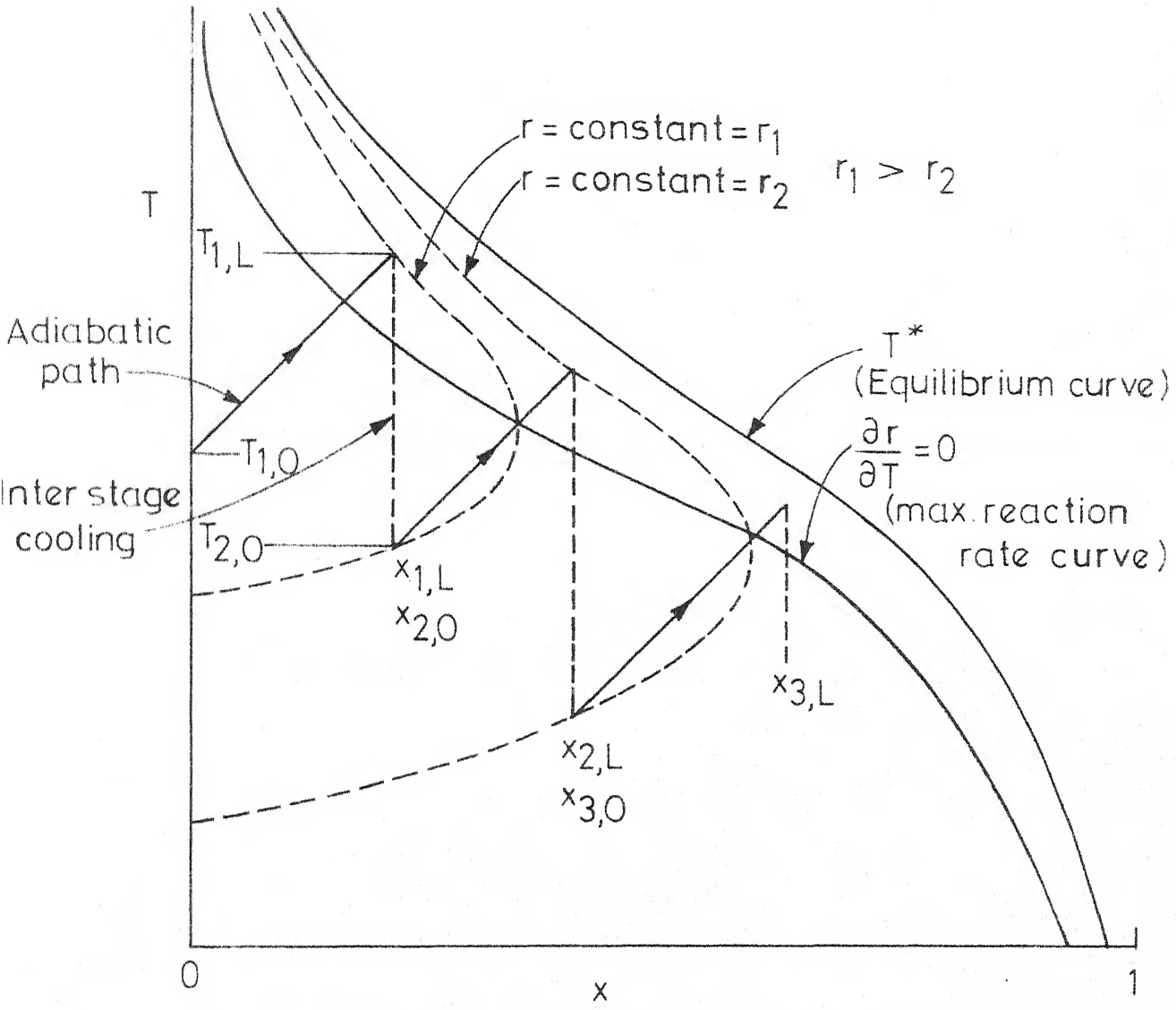

Fig. 2-3 - Illustration of the optimum conditions.

CHAPTER 3

LITERATURE SURVEY

Chemical Reaction Rate of the Shift Reaction:

A number of workers have studied the behaviour of the water-gas shift reaction over high temperature iron-based shift catalyst. Various forms of empirical rate equations have been suggested by different authors. A few investigators have proposed and tested reaction models also.

Laupichler[5] used a simple bimolecular expression for determining the rate of the shift reaction in the homogeneous phase. In the process of an industrial-scale production of hydrogen, in which a large excess of steam is added to the dry gas, the change in concentration of water vapor can be neglected during the course of reaction. Based on this fact, Laupichler justified the use of a pseudo first order rate equation in carbon monoxide in place of second order rate equation.

It was considered that the effect of the catalyst was to increase the rate of conversion without changing the form of the rate expression. The effect of external diffusion was also taken into consideration.

Padovani and Lotteri[6] also assumed a second order expression for the forward rate of reaction, r_f, i.e.

$$r_f = k \; p_{CO} \; p_{H_2O} \qquad (3.1)$$

Where

k = reaction rate constant

p_i = partial pressure of the component i

Kulkova and Temkin[7] found that the following rate expression adequately covered the experimental data.

$$r = k\, p_{CO} \left(p_{H_2O}/p_{H_2} \right)^{b} - k'\, p_{CO_2} (p_{H_2}/p_{H_2O})^{1-b} \qquad (3.2)$$

with, $b = 0.44$ to 0.50

According to this equation, H_2 has a retarding effect on the rate of forward reaction, whereas CO_2 has no such influence.

Atwood[8] and Mars[9] applied a first order kinetic expression of the following type:

$$r = k \left(p_{CO} - p^{*}_{CO} \right) \qquad (3.3)$$

Where

p^{*}_{CO} = partial pressure of CO at equilibrium.

Popov[10] used an unpromoted iron, oxide catalyst and found that the rate was first order with respect to CO and zero order with respect to H_2O. At temperatures above 400°C, the reaction order with respect to H_2O changed to 0.5.

Barkley and coworkers[11] studied the kinetics of the reverse shift reaction using the Fe_2O_3 - CuO shift catalyst and obtained the following rate equation:

$$r = k \frac{p_{CO_2} p_{H_2} - K' p_{CO} p_{H_2O}}{1 + K_{CO} p_{CO} + K_{CO_2} p_{CO_2}} \qquad (3.4)$$

It is not very clear if this equation will hold for the water-gas shift reaction also.

Kodama[12] studied reaction rates over a coprecipitated Fe_2O_3 - Cr_2O_3 catalyst, and arrived at an equation of the type:

$$r = k \frac{p_{CO} p_{H_2O} - K' p_{CO_2} p_{H_2}}{p_{CO_2} + K_{H_2O} p_{H_2O}} \qquad (3.5)$$

In this study, the contact times were far shorter than those used in industrial reactors.

Later Kodama[13] using an industrial catalyst of somewhat different composition arrived at the following rate expression:

$$r = k \frac{p_{CO} p_{H_2O} - K' p_{CO_2} p_{H_2}}{1 + K_{CO} p_{CO} + K_{H_2O} p_{H_2O} + K_{H_2} p_{H_2} + K_{CO_2} p_{CO_2}} \qquad (3.6)$$

The latter equation was found to be valid over larger concentration ranges than the former.

Bortolini[14] studied the shift reaction at atmospheric pressure and at relatively high temperatures using a commercial Fe_2O_3 - Cr_2O_3 catalyst. It was found that at temperatures of

about 500°C and higher, the reaction rate is controlled by the external diffusion.

Stelling and Krusenstierna[15] investigated the reaction rate in the presence of an iron-oxide catalyst. It was found that even very small amounts of CO_2 have a strong inhibiting effect on the forward rate whereas H_2 does not take part in the reaction. Their rate equation for the forward reaction is:

$$r_f = k \frac{p_{CO}\, p_{H_2O}}{p_{CO_2} + K_{H_2O}\, p_{H_2O}} \qquad (3.7)$$

Kirillov[16] used an industrial Fe_2O_3 catalyst and developed the following rate equation:

$$r = k\, p_{H_2O} \left(\frac{p_{CO}}{p_{CO_2}} \right)^{1/2} - k'\, p_{H_2} \left(\frac{p_{CO_2}}{p_{CO}} \right)^{1/2} \qquad (3.8)$$

Atroshchenko and Bibr[17] studied the reaction rate over a commercial catalyst containing MgO and Fe_2O_3 as the major constituents, in the pressure range of 6 to 21 atm. The data was correlated by the equation:

$$r = k \frac{p_{CO} - p^*_{CO}}{p_{H_2}} \left(p_{H_2O}\right)^{1/2} \qquad (3.9)$$

Hulburt and Srinivasan[18] used a commercial promoted iron oxide catalyst and arrived at the following equation for the forward rate at 350°C:

$$r_f = \frac{0.2107\ p_{H_2O}}{1+1.063\ \frac{p_{H_2O}}{p_{H_2}}} \qquad (3.10)$$

According to this expression, reaction rate is not affected by p_{CO} and p_{CO_2} whereas it increases with p_{H_2}.

Bohlbro[19] investigated the kinetics of the shift reaction at atmospheric pressure over an iron-oxide chromium oxide catalyst, in the temperature range of 330-500°C. It was observed that the rate is independent of the hydrogen partial pressure, whereas an increase of carbon dioxide partial pressure serves to decrease the reaction rate. He proposed an empirical rate equation of the exponential type for the forward reaction.

$$r_f = k(p_{CO})^l \cdot (p_{H_2O})^m \cdot (p_{CO_2})^n \cdot (p_{H_2})^q \qquad (3.11)$$

The exponents were found to vary within certain ranges of temperature. The following ranges were obtained for the exponents:

$l = 0.80$ to 1.00

$m = 0.20$ to 0.35

$n = -0.65$ to -0.50

$q = 0$

Atroshchenko and coworkers[20] also used the same

exponential type rate equation. The investigation was performed at 300°C and 460°C over an iron-chromium oxide catalyst, and different values for the exponents were obtained at the two temperatures.

Later Goodridge[21] also investigated the same exponential rate expression using several iron base shift catalysts, in the temperature range of 350-430°C. The exponential constants varied significantly as a function of temperature as well as with each of the catalyst. His study was, however, in agreement with Bohlbro's work for the same catalyst.

Moe[22] found that Laupichler's [5] second order expression was applicable for calculation of industrial converters using the iron oxide shift catalysts with Cr_2O_3 as a promoter. The rate equation can be written as:

$$r = k_2 \left[y_{CO} \cdot y_{H_2O} - \frac{y_{CO_2} \cdot y_{H_2}}{K} \right] \qquad (3.12)$$

Where,

y_i = mole fraction of component i

k_2 = second order rate constant for the forward reaction

K = Equilibrium constant for water gas shift reaction

The rate constant was further modified to consider the effect of factors like size of the catalyst particles, period of run and operating pressure.

From the investigations of different workers, it is evident that even with extensive kinetic studies for the shift reaction, there seems to be little agreement about the exact form of the rate equation.

CHAPTER 4

THE SIMULATION MODEL

The simulation model is developed by taking into consideration all the physical and chemical processes occurring in the reactor based on certain simplifying assumptions.

The following assumptions are made in deriving the model.

1. The bed is completely adiabatic.
2. The composition and temperature in the radial direction are uniform. Because of the adiabatic nature of the bed, this assumption is justified.
3. The velocity profile is flat at any cross section. A large ratio of bed diameter to the catalyst pellet diameter implies that the velocity profile is essentially uniform along the bed diameter.
4. There is negligible axial diffusion in the bed.
5. The reactor is in a steady-state.
6. Pressure is constant over the length of the reactor.

The assumptions 2, 3 and 4 constitute the plug-flow

reactor model.

I. Material Balance:

Assuming CO as the guide-species, a material balance over a cross section of the catalyst bed leads to

$$F \cdot y_{f,CO} \cdot dx = r \cdot dV \qquad (4.1)$$

Where,

F = Total flow of gas mixture, $Nm^3/hr.$

$y_{f,i}$ = Mole fraction of component i in feed stream.

x = Degree of conversion of CO.

r = Overall rate of reaction of CO, $\frac{Nm^3 \text{ of CO-converted}}{(m^3 \text{ bed volume})(hr)}$

V = Volume of reactor bed, m^3.

II. Energy Balance:

The energy balance in case of adiabatic operation is obtained by equating the heat of reaction term to the sum of the sensible heat gain for the gases. For a system with no change in number of moles on reaction, this yields

$$\left[\sum_i y_i \, C_{p_i}(T,P)\right] dT = \left[-\Delta H_R(T,P)\right] y_{f,CO} \cdot dx \qquad (4.2)$$

Where,

y_i = mole fraction of component i

ΔH_R = Heat of reaction, cal/gmmole of CO

C_{p_i} = molal heat capacity of component i, cal/(gmmole)-(°K)

T = Absolute temperature, °K

P = Total pressure, atm.

The summation in the energy balance equation is over all the reactants and products present in the reaction mixture.

The nonideal behaviour of the gases has been considered and, therefore, the values of heat capacities $(C_P)_i$ and heat of reaction ΔH_R are dependent on temperature and pressure. The specific heats are expressed by Hougen and Watson[23] as polynomials in T; and their pressure dependence has been obtained by using data[24] at different pressures (details are shown in Appendix II). Table 4.1 lists the heat capacity relationships for various gases; the pressure dependency for gases other than steam is negligible.

TABLE 4.1: RELATIONSHIPS FOR HEAT CAPACITIES OF VARIOUS GASES

(T in °K ; C_P in g-cal/(gmmole)(°K))

	Gas	Heat Capacity Equation*
1.	H_2	$(C_P)_1 = 6.946 - 0.196 \times 10^{-3}T + 0.4757 \times 10^{-6} T^2$
2.	CO	$(C_P)_2 = 6.350 + 1.811 \times 10^{-3}T - 0.2675 \times 10^{-6} T^2$
3.	CO_2	$(C_P)_3 = 6.339 + 10.14 \times 10^{-3}T - 3.415 \times 10^{-6} T^2$
4.	CH_4	$(C_P)_4 = 3.204 + 18.41 \times 10^{-3}T - 4.48 \times 10^{-6} T^2$
5.	N_2	$(C_P)_5 = 6.457 + 1.389 \times 10^{-3}T - 0.069 \times 10^{-6} T^2$
6.	A	$(C_P)_6 = 4.97$
7.	H_2O	$(C_P)_7 = 7.136 + 2.640 \times 10^{-3}T + 0.0459 \times 10^{-6} T^2 + 0.63 \times 10^{14} P^{1.29}/T^{5.56}$

*Pressure range 1 to 40 atm.

The heat of reaction has also been expressed as a function of temperature and pressure (Details shown in Appendix II) and the resulting expression is

$$\Delta H_R = \left[\Delta a.T + \frac{\Delta b}{2} T^2 + \frac{\Delta c}{3} T^3 + 13.82*10^{12} P^{1.29}T^{-4.56}\right] - 2.96 P^{1.29} - 0.933*10^4 \exp(-0.9354*10^{-3}P) - 672.47 \quad (4.3)$$

With

$\Delta a = -0.201$

$\Delta b = 5.493 * 10^{-3}$

$\Delta c = -2.7177 * 10^{-6}$

The above equation is valid in the normal operating range of shift reaction (Temperature range 600 to 800°K and pressure range 1 to 40 atm.).

III. Kinetics of the Shift Reaction

As appears from the literature survey (Chapter 3), a generally accepted kinetic expression for the shift reaction does not exist. It is quite justifiable, therefore, to make use of a kinetic equation which is both simple and sufficiently accurate at least for industrial purposes. Thus the rate equation chosen for developing the simulation model is the second order rate expression[5,22] for which a pseudo first order equation is a reasonable approximation when steam is present in considerable excess. The derivation is shown in

Appendix III. The pseudo-first order rate expression can be written as

$$r = k_1 (y_{CO} - y^*_{CO}) \qquad (4.4)$$

with

$$k_1 = k_2 \bar{y}_{H_2O} \qquad (4.4a)$$

Where

y_{CO} = mole fraction of CO

y^*_{CO} = equilibrium mole fraction of CO

k_2, k_1 = second order and pseudo first order rate constants respectively,

$\bar{y}_{H_2O}$ = mean value for the mole fraction of $H_2O(g)$.

(It will often be satisfactory to assume that a given bed operates at the mean of the inlet and outlet steam concentration. However, for more accurate calculations, a stepwise procedure may be adopted where the mean concentration is estimated over small increments of reactor bed).

It has been shown by Ruthven[25] that under normal operating conditions, external mass transfer resistance is usually negligible in an industrial shift converter. It appears that under most conditions the major resistance is due to pore diffusion of carbon monoxide. The assumption of thermal equilibrium between the catalyst and gas with a uniform temperature throughout the catalyst pellet appears to be justified[26].

The pore diffusion tends to alter the value of the effective rate of reaction and this modification can be taken into account by introducing a suitable effectiveness factor, E. For the direct evaluation of E in case of (pseudo) first order reaction, the correlations proposed by Thiele[27] can be used. According to him, in case of a first order reaction taking place in an isothermal catalyst particle, the influence of a restricted internal diffusion on the reaction rate is governed by a dimensionless modulus m. Using the formulation of Hoogschagen[28], the dimensionless modulus has the form

$$m = \frac{D_P}{2}\sqrt{\frac{k_{v_1}}{D_{eff}}} \qquad (4.5)$$

in which

D_P = catalyst particle diameter, cm.

kv_1 = intrinsic catalyst activity, sec^{-1}

D_{eff} = effective diffusion coefficient in the porous catalyst under reaction conditions, $cm^2/sec.$

Disregarding the change of D_{eff} with conversion, the value of m is independent of concentration for a first order reaction.

From the solution of the diffusional equation (2.4), the effectiveness factor, E, of the catalyst pellet can be determined and this leads to the relation

$$E = \frac{3}{m}\left(\frac{1}{\tanh\ m} - \frac{1}{m}\right) \qquad (4.6)$$

The effective particle diameter, D_P, can be calculated from the formula [28]

$$D_P = 6\ V_P/A_P \qquad (4.7)$$

in which A_P is the gross exterior surface area and V_P is the volume. For spheres this formula gives the actual diameter.

The apparent reaction rate constant, ko_1, based on unit catalyst bed volume is ordinarily different from kv_1 and can be expressed as [29,26]

$$ko_1 = kv_1\ (1-e)\ E \qquad (4.8)$$

Here e is the voidage of catalyst bed and its value can be taken as 0.4 for uniformly sized particles [25].

For computing the apparent activity, ka_1, defined with respect to space velocity measured under standard conditions, usually N.T.P., the relation used is [26]

$$ka_1 = ko_1 \cdot 3600 \cdot \left(\frac{273}{T}\right).P \qquad (4.9)$$

The units of ko_1 and ka_1 in this equation being Sec^{-1} and hr^{-1} respectively.

The question of the effective diffusion coefficient in ferric oxide-chromic oxide shift catalysts has been discussed by Hoogschagen[28]. It has been shown that for the catalyst tablets prepared by compression of a powder, the diffusion through the highly heterogeneous pore system predominantly has the character of normal gas diffusion. The value of effective

diffusion coefficient, D_{eff}, was estimated to be 0.039 sq. cm/sec. for CO at 1 atm. and 350°C. It can be assumed to a good approximation that D_{eff} does not change with the degree of conversion over the range of gas compositions encountered in practical shift converters[26]. Assuming the same effective diffusivity data to be valid for the present catalyst, the effective diffusivity at other pressures and temperatures may then be calculated from the expression[29,26]

$$D_{eff} = \left(\frac{0.039}{P}\right)\left(\frac{T}{623}\right)^{1.5} \quad cm^2/sec \qquad (4.10)$$

The value of D_{eff} from this equation can be used for calculating the Thiele modulus and therefore the effectiveness factor.

The values of the kinetic parameters have been evaluated using the pilot plant kinetic-data reported by Chandra etal[30] for the FCI H.T. Shift Catalyst. The pilot plant data have been obtained using 6 mm dia.* 3 mm. long catalyst tablets. Use of equation (4.7) gives D_p = 0.45 cm. for which the pore diffusional resistance must be significant.

When pore diffusional resistance is important, Eqn.(4.6) simplifies to give

$$E \simeq \frac{3}{m}\left(1 - \frac{1}{m}\right) \qquad (4.11)$$

Valid for $m > \sim 3$, $\qquad E < \frac{2}{3}$

Eqns. (4.8), (4.9) and (4.11) can be combined to give

$$ka_1 \simeq \frac{6}{D_P}\left(\sqrt{kv_1 \cdot D_{eff}} - \frac{2\,D_{eff}}{D_P}\right)(1-e).3600\left(\frac{273}{T}\right)P \quad (4.12)$$

Eqns. (4.10) and (4.12) can then be used for evaluating the value of kv_1 at a given pressure and temperature from the value of ka_1 which is available from pilot plant data.

III.A Calculation of Intrinsic Activation Energy:

The temperature dependence of the intrinsic rate constant, kv_1, can be expressed by a simple Arrhenius relationship,

$$kv_1 = Z_1\, e^{-E_a/RT} \quad (4.13)$$

Where,

E_a = intrinsic activation energy, gm-cal/gm-mole

R = gas constant = 1.987 gm-cal/gm-mole °K

T = Temperature, °K

Z_1 = Pre exponential factor of intrinsic rate constant, sec^{-1}

The pilot plant data at two different catalyst life-periods and pressures have been used for determining the value of E_a. The results calculated are shown in Tables 4.2 and 4.3.

By plotting log kv_1 versus 1/T, straight lines are obtained as shown in Fig. 4.1 and 4.2. From the slope of the straight line, the value of E_a/R obtained is $9.33 * 10^3$ and $9.12 * 10^3$ respectively, which are practically identical.

From these the average intrinsic activation energy has been calculated to be $18.330 * 10^3$ gm cal/gm-mole.

This value for the intrinsic activation energy corresponds fairly well with the latest values of $21.4*10^3$ to $27.3*10^3$ cal/mole calculated by Ruthven[26] for various commercial shift catalysts.

TABLE 4.2: CALCULATION OF INTRINSIC CATALYST ACTIVITY AT VARIOUS REACTION TEMPERATURES

No.	Temperature °C	Avg. value of experimentally determined rate constant ka_1, hr^{-1}	$\frac{1}{T\ °K}$	Calculated values of intrinsic rate constant kv_1, sec^{-1}
1.	480	$0.3235 * 10^5$	$1.328 * 10^{-3}$	8.36
2.	460	$0.25965* 10^5$	$1.364 * 10^{-3}$	5.48
3.	440	$0.2215 * 10^5$	$1.403 * 10^{-3}$	4.05
4.	435	$0.2340 * 10^5$	$1.412 * 10^{-3}$	4.435
5.	420	$0.18517* 10^5$	$1.443 * 10^{-3}$	2.88
6.	415	$0.1670 * 10^5$	$1.453 * 10^{-3}$	2.38

Pilot plant data corresponds to:

Catalyst life period 1605.5 hrs to 1662.0 hrs and

Pressure 26 kg/cm^2 abs.

TABLE 4.3: CALCULATION OF INTRINSIC CATALYST ACTIVITY AT VARIOUS REACTION TEMPERATURES

No.	Temperature °C	Avg. value of experimentally determined rate constant ka_1, hr^{-1}	$\frac{1}{T\ °K}$	Calculated value of intrinsic rate constant kv_1, sec^{-1}
1.	435	$0.3070 * 10^5$	$1.412 * 10^{-3}$	9.06
2.	430	$0.2775 * 10^5$	$1.422 * 10^{-3}$	7.715
3.	415	$0.2560 * 10^5$	$1.453 * 10^{-3}$	6.37
4.	412	$0.2460 * 10^5$	$1.460 * 10^{-3}$	5.90
5.	410	$0.2367 * 10^5$	$1.464 * 10^{-3}$	5.50
6.	408	$0.2115 * 10^5$	$1.468 * 10^{-3}$	4.47
7.	405	$0.2160 * 10^5$	$1.475 * 10^{-3}$	4.63
8.	400	$0.2242 * 10^5$	$1.486 * 10^{-3}$	4.93
9.	395	$0.1948 * 10^5$	$1.497 * 10^{-3}$	3.815
10.	390	$0.1840 * 10^5$	$1.508 * 10^{-3}$	3.42
11.	385	$0.2080 * 10^5$	$1.520 * 10^{-3}$	4.25
12.	380	$0.1745 * 10^5$	$1.531 * 10^{-3}$	3.09
13.	375	$0.1790 * 10^5$	$1.543 * 10^{-3}$	3.21
14.	365	$0.1649 * 10^5$	$1.567 * 10^{-3}$	2.75
15.	355	$0.1650 * 10^5$	$1.592 * 10^{-3}$	2.73

Pilot plant data corresponds to:

Catalyst life period 1114.0 to 1172.5 hrs.

and Pressure 21 kg/cm^2 abs.

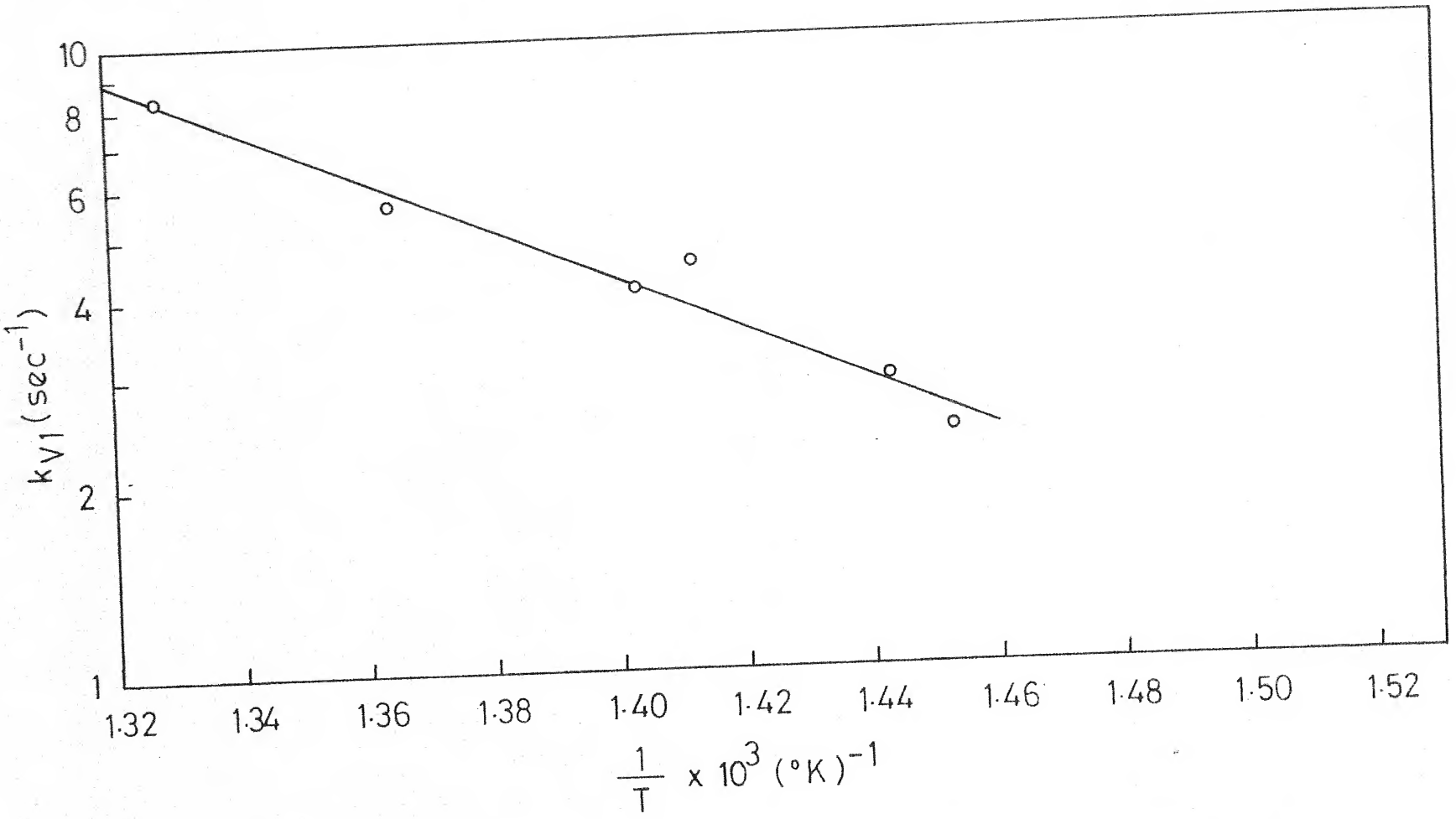

Fig. 4·1 - Arrhenius plot of intrinsic rate constant.
(Data from Table 4·2)

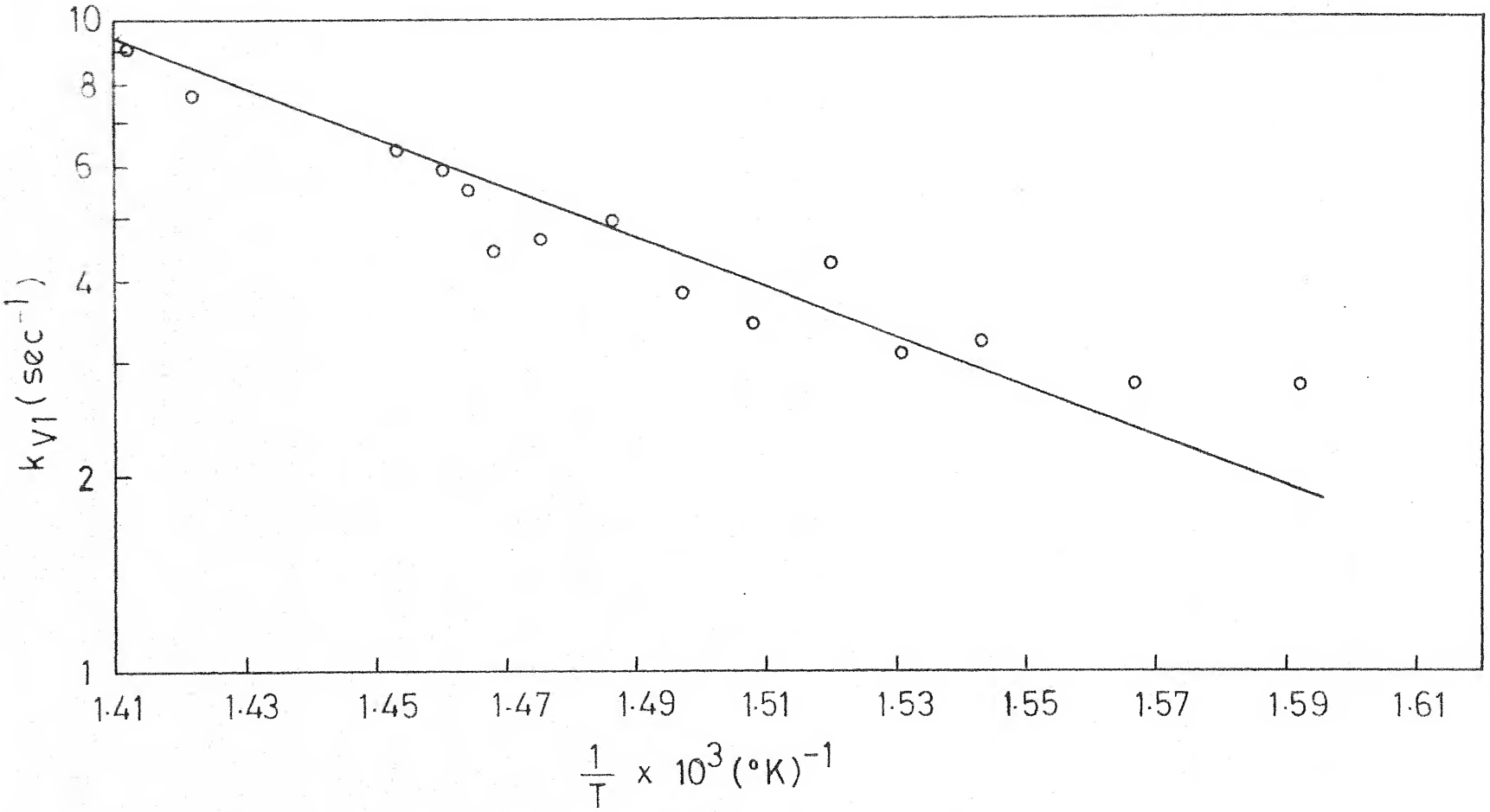

Fig. 4·2 - Arrhenius plot of intrinsic rate constant.
(Data from Table 4·3)

III.B Effect of Pressure on Catalyst Activity

Pressure serves to increase the activity of the shift catalyst. The increase in the activity with pressure seems to be related to the availability of the internal surface area[22].

To evaluate the dependence of the intrinsic rate constant on total pressure, an empirical equation has been fitted in the pressure range of 6-26 kg/cm^2 abs. The same rate equation is assumed to be valid over the entire range, As all of the values of ka_1 available for studying the effect of pressure are not exactly at the same temperature, a correction is necessary for the effect of varying temperature. Using the value of $E_a = 18.330 * 10^3$ gm cal/gm mole, the calculated values of kv_1 have, therefore, been corrected for deviations of temperature from the level of 390°C. For fitting the empirical equation, the values of $(kv_1 * P)$ have been calculated at 390°C. The results are shown in Table 4.4.

A plot of log $(kv_1 * P)$ against 1/P is represented in Fig. 4.3. A linear relationship is obtained which means that the relation between kv_1 and P in the pressure range of 6-26 Kg/cm^2 abs. can be expressed by

$$kv_1 \propto \frac{\theta^{-F_a/P}}{P} \qquad (4.14)$$

and the slope obtained from the plot gives

$$F_a = 13.430 \qquad \text{(when P = Kg/cm}^2\text{ abs.)}$$

(For extrapolation purposes, the same relationship may be assumed to be valid at least upto a pressure of 30 Kg/cm^2abs.)

TABLE 4.4: EVALUATION OF THE PRESSURE DEPENDENCE OF INTRINSIC CATALYST ACTIVITY

No.	Pressure P, Kg/cm^2 abs.	Temperature °C	Avg. value of experimentally determined rate constant ka_1, hr^{-1}	1/P	Average Calculated value of $(kv_1 * P)$ at 390°C Sec^{-1} Kg/cm^2
1.	26.0	380	$0.2090 * 10^5$	0.0385	110.82
2.	21.0	380	$0.1970 * 10^5$	0.0476	91.58
		390	$0.2001 * 10^5$		
3.		390	$0.1930 * 10^5$		
	16.0	390	$0.1520 * 10^5$	0.0625	62.11
		390	$0.1610 * 10^5$		
4.		390	$0.1592 * 10^5$		
	11.0	388	$0.1349 * 10^5$	0.0909	48.39
		380	$0.1302 * 10^5$		
		375	$0.1199 * 10^5$		
5.	6.0	375	$0.6750 * 10^4$	0.1667	18.44

Pilot plant data corresponds to:

Catalyst life period 266.0 to 378.5 hrs.

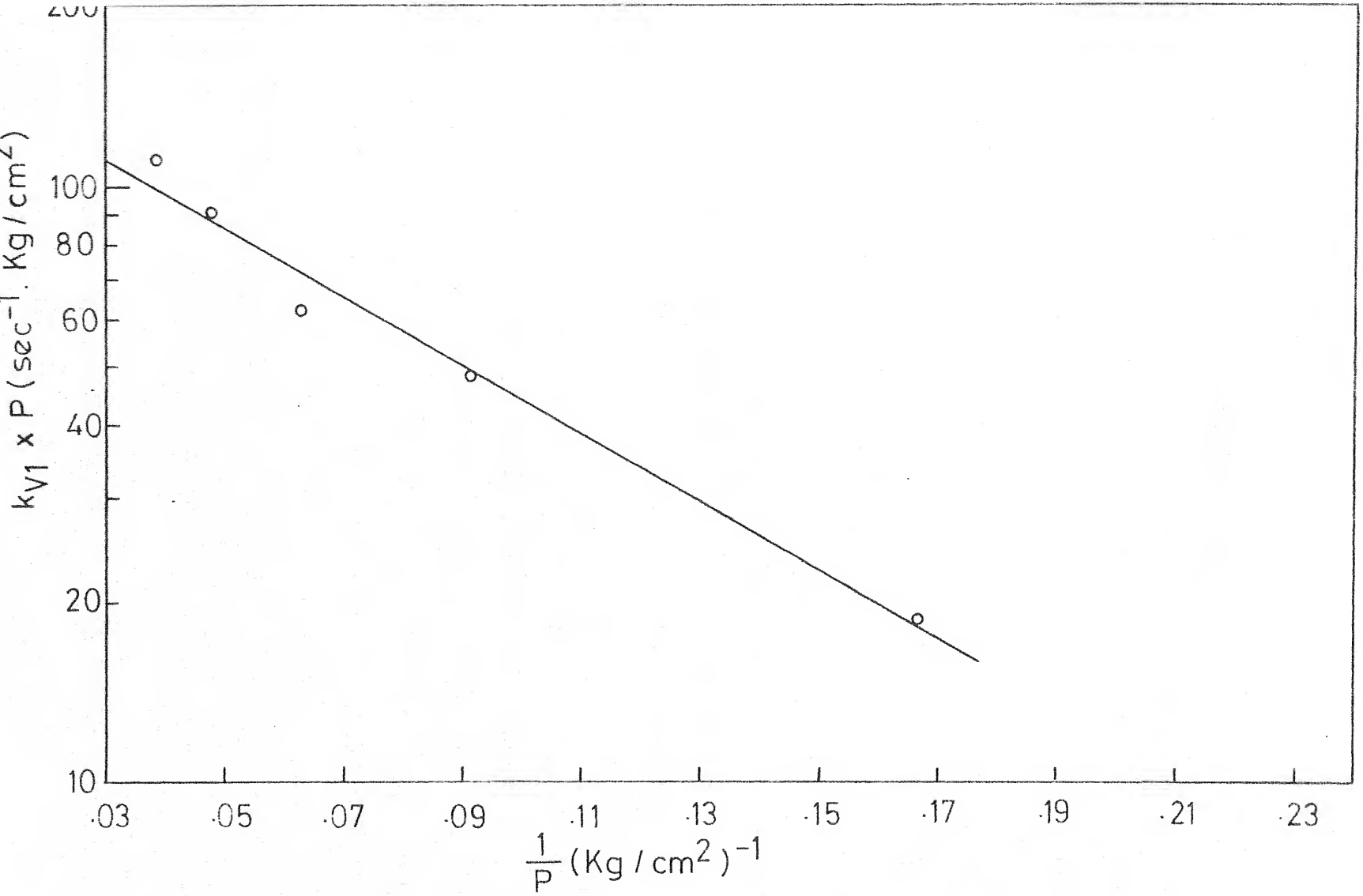

Fig. 4·3 - Plot of $\log(k_{V1} \times P)$ vs. $1/P$.

III.C Effect of Ageing on Catalyst Activity

The activity of the freshly prepared shift catalyst undergoes a rapid decline during the first few hours of operation and thereafter, the rate of decline becomes more gradual. The catalyst apparently sinters, thereby resulting in a decrease in surface area[22]. This sintering phenomenon is the result of a combined effect of catalyst-age and reaction temperature[9]. But there appears to be no simple relationship between catalyst activity and these factors. It is rather difficult to individually assess these factors and correlate them with efficiency of catalyst[31].

Mahapatra and coworkers[31] have computed the fall of catalyst activity with time for the H.T. shift catalyst using the data of a commercial reactor operating in the temperature range of 350-410°C. They obtained a straight line relationship on a logarithmic plot (shown in Appendix IV) of fractional activity against time of operation. Using this linear relationship, the dependence of the ageing factor (loss of original activity due to time on stream) on time can be expressed by

$$A_f = t^{-0.079} \qquad (t \geq 1) \qquad (4.15)$$

where

A_f = aging factor

t = time on stream (days)

III.D Influence of H_2S on Catalyst Activity

The activity of a shift catalyst is lowered by gases containing H_2S which reacts with the iron oxide to form iron sulfide[32]. In industrial practice the CO - Conversion is performed without or with different concentrations of H_2S as impurity, depending on the source of the feed gas.

Although the effect of H_2S on catalyst activity is quite important, not much work has been published in this field. To evaluate the influence of H_2S, the use of an approximate sulfur-factor is necessitated in absence of any data for the present catalyst. Making use of the data from other sources[33], a plot (shown in appendix IV) of sulfur factor, f_s, against log (H_2S) has been found to give a straight line. The variation of f_s with concentration of H_2S can then be expressed by the relation

$$f_s = - 0,276 \log_{10} (H_2S) + 1.127 \qquad (4.16)$$

where

(H_2S) = concentration of H_2S in ppm. (dry basis).

At the point where $f_s=1$, the corresponding value of (H_2S) determined from the plot is 2.7 ppm which is somewhat uncertain. However, this value may be considered as being practically equal to zero.

Finally it may be mentioned that the use of eqn.(4.16) for determining the sulfur factor is clearly an approximation. To calculate accurate factors would require experimental data

on the catalyst in the reactor, which are not available.

Combining eqns. (4.13) to (4.16), the final expression for the intrinsic reaction rate constant may be written as

$$kv_1 = Z' e^{-E_a/RT} \cdot \frac{e^{-F_a/P}}{P} \cdot A_f \cdot f_s \qquad (4.17)$$

with

$$Z_1 = Z' \frac{e^{-F_a/P}}{P} \cdot A_f \cdot f_s$$

Use of eqn.(4.4a) then gives

$$kv_2 = Z_o \cdot e^{-E_a/RT} \cdot \frac{e^{-F_a/P}}{P} \cdot A_f \cdot f_s \qquad (4.18)$$

with

$$Z_o = \frac{Z'}{\bar{y}_{H_2O}} \qquad (4.18a)$$

Evaluation of Z_o

Use of eqn.(4.13) and Fig. 4.1 has been made to calculate

$$Z_1 = 1.983 * 10^6 \text{ sec}^{-1}$$

corresponding to the following conditions:

$t = (1605.5 + 1662.0)/2$ hrs. = 68 days

$P = 26$ kg/cm^2 abs.

$\bar{y}_{H_2O} = 0.4490$

$(H_2S) = 60$ ppm (dry basis)

The values of $\bar{y}_{H_2O}$ and (H_2S) are available along with other pilot plant data.

Using these conditions,

$$\frac{e^{-F_a/P}}{P} = 0.023$$

$$A_f = 0.716$$

$$f_s = 0.637$$

Then use of eqns. (4.13) and (4.17) gives

$$Z' = \frac{1.983 * 10^6}{0.023 * 0.716 * 0.637} = 1.895 * 10^8 \text{ sec}^{-1}$$

The value of Z_o can then be evaluated from eqn. (4.18a),

$$Z_o = \frac{1.895 * 10^8}{0.4490}$$

$$= 4.22 * 10^8 \text{ sec}^{-1}.$$

Eqns.(4.17) and (4.18) can then be used to calculate the value of kv_1 at a given set of conditions $\left[\bar{y}_{H_2O}, T, P, t \text{ and } (H_2S)\right]$.

The value of E can be computed using eqns. (4.5) to (4.7) and (4.10) for a given catalyst size.(To give an idea about the magnitude of effectiveness factor, the values of E obtained at different positions in the catalyst bed are shown in Appendix IV). By inserting the value of E and kv_1, the apparent rate constant ka_1 is calculated by means of eqns. (4.8) and (4.9). To obtain the corresponding value of overall reaction rate, r, to be inserted in the material balance eqn.(4.1), use is to be made of eqn.(4.4) with $k_1 = ka_1$.

IV. The Equilibrium Conversion

The equilibrium conversion of CO can be evaluated from the value of equilibrium constant for the shift reaction. The equilibrium constant, K, has been calculated from the thermodynamic considerations using entropy data and the relation thus developed is:

$$\ln K = -\frac{1}{RT}\left[-9998.220 + (\Delta a + 10.414)T - \frac{\Delta b}{2}T^2 - \frac{\Delta c T^3}{6} - \Delta a . T . \ln T\right] \qquad (4.19)$$

The details of the derivation of this equation are described in Appendix V. Some of the calculated values for K are listed in Table 4.5. These are closely in agreement with the values reported by Lavrov[34].

TABLE 4.5: EQUILIBRIUM CONSTANT VALUES FOR THE SHIFT REACTION

T, °K	Equilibrium Constant K	
	Calculated from Eqn.(4.19)	Reported by Lavrov
600	28.410	28.274
700	9.409	9.4126
800	4.194	4.2191
900	2.276	2.2972

For computing the equilibrium conversion, the composition ratio K_y is related to the equilibrium constant by the relation[35]:

$$K = P^{\Delta n} \; K_{\alpha} \; K_y \qquad (4.20)$$

Where

Δn = change in the number of moles as a result of the reaction.

K_y = composition ratio defined in terms of mole fractions

$$= \frac{y^*_{CO_2} \; y^*_{H_2}}{y^*_{CO} \; y^*_{H_2O}} \qquad (4.21)$$

Defining,

$$y_{conv} = y_{f,CO} - y^*_{CO}$$

$$K_y = \frac{(y_{f,CO_2} + y_{conv})\,(y_{f,H_2} + y_{conv})}{(y_{f,CO} - y_{conv})\,(y_{f,H_2O} - y_{conv})} \qquad (4.21a)$$

$$K_{\alpha} = \frac{\left(\frac{f}{P}\right)_{CO_2} \; \left(\frac{f}{P}\right)_{H_2}}{(f/P)_{CO} \; (f/P)_{H_2O}} \qquad (4.22)$$

in which

f = fugacity of the pure component at the temperature and pressure of the mixture.

For shift reaction, since there is no change in number of moles during the reaction,

$$\Delta n = 0$$

Using the fugacity chart[35] to find the f/P ratio for each component, the values of K_{α} have been calculated at several combinations of temperature and pressure in the normal operating

range of shift reaction . The different values of K_{α} have been found to be very close to unity, so that

$$K_{\alpha} \simeq 1.0$$

Hence eqn.(4.20) becomes:

$$K_y \simeq K \qquad (4.20a)$$

Eqns. (4.20a) and (4.21a) can then be combined together to give the value of y_{conv} and thus y^*_{CO} at any desired temperature from the given feed gas composition.

V. Stoichiometric Relations

The stoichiometric relations lead to the expressions for y_i as follows:

$$y_{H_2} = y_{f,H_2} + y_{f,CO} \cdot x \qquad (4.23)$$

$$y_{CO} = y_{f,CO} - y_{f,CO} \cdot x \qquad (4.24)$$

$$y_{CO_2} = y_{f,CO_2} + y_{f,CO} \cdot x \qquad (4.25)$$

$$y_{H_2O} = y_{f,H_2O} - y_{f,CO} \cdot x \qquad (4.26)$$

$$y_{inert} = y_{f,\ inert} \qquad (4.27)$$

Eqns. (4.1) to (4.10) and (4.15) to (4.27) thus constitute the simulation model for the shift reactor.

The inlet temperature and flow rate of each component at the entrance of each bed (V=0) constitute the boundary conditions for the system.

VI. Numerical Solution

The simulation equations comprise a set of coupled and

nonlinear first-order ordinary differential equations which cannot be solved analytically. The equations have therefore been solved numerically using fourth-order Runge-Kutta[36] integration technique starting at the bed inlet and proceeding stepwise, the computation cycle is continued until known value of the volume at the bed exit is reached. In all cases the maximum step size is chosen subject to the limitation of relative error specified (errors of less than 0.1% in temperature have been allowed).

The solution to the simulation equations has been carried out on IBM 7044 computer using Fortran IV language for programming.

VII. Comparison of the Simulation Model with Plant Data

A comparison of the model production with actual plant measurements is shown in Table 4.6. (A complete list of plant data has been presented in Appendix IV). Fig. 4.4 and 4.5 show the calculated temperature and conversion profiles in the reactor beds.

The agreement between plant data and model results is seen to be quite satisfactory. An exact matching of the two may not be possible in view of the errors in plant measurements and the experimental uncertainty in the kinetic data.

TABLE 4.6: COMPARISON OF REACTOR SIMULATION WITH PLANT RESULTS

Parameter	Simulation			Plant Measurement		
	1st bed	2nd bed	3rd bed	1st bed	2nd bed	3rd bed
%composition of exit-gas						
H_2	62.56	65.08	65.51	59.6	63.1	64.6
CO	12.48	4.90	3.62	14.2	4.8	3.6
CO_2	22.56	27.78	28.66	23.0	29.4	30.0
N_2+CH_4+A	2.40	2.24	2.21	3.2	2.7	1.8
Temperatures, °C (In/Out)	351/475	400/444	406/414	351/460	400/459	406/415

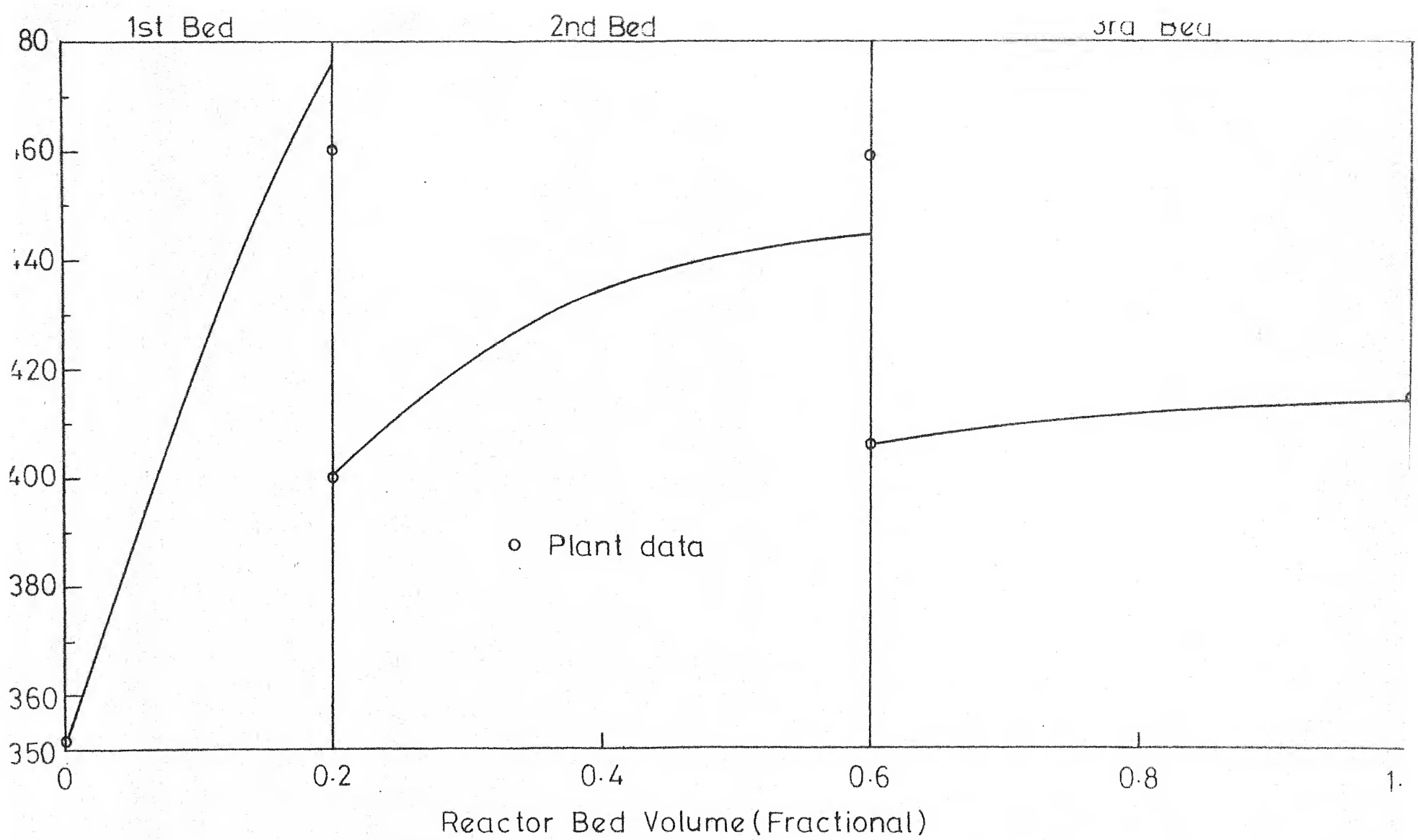

Fig. 4 .4 - Temperature profiles calculated in the reactor beds.

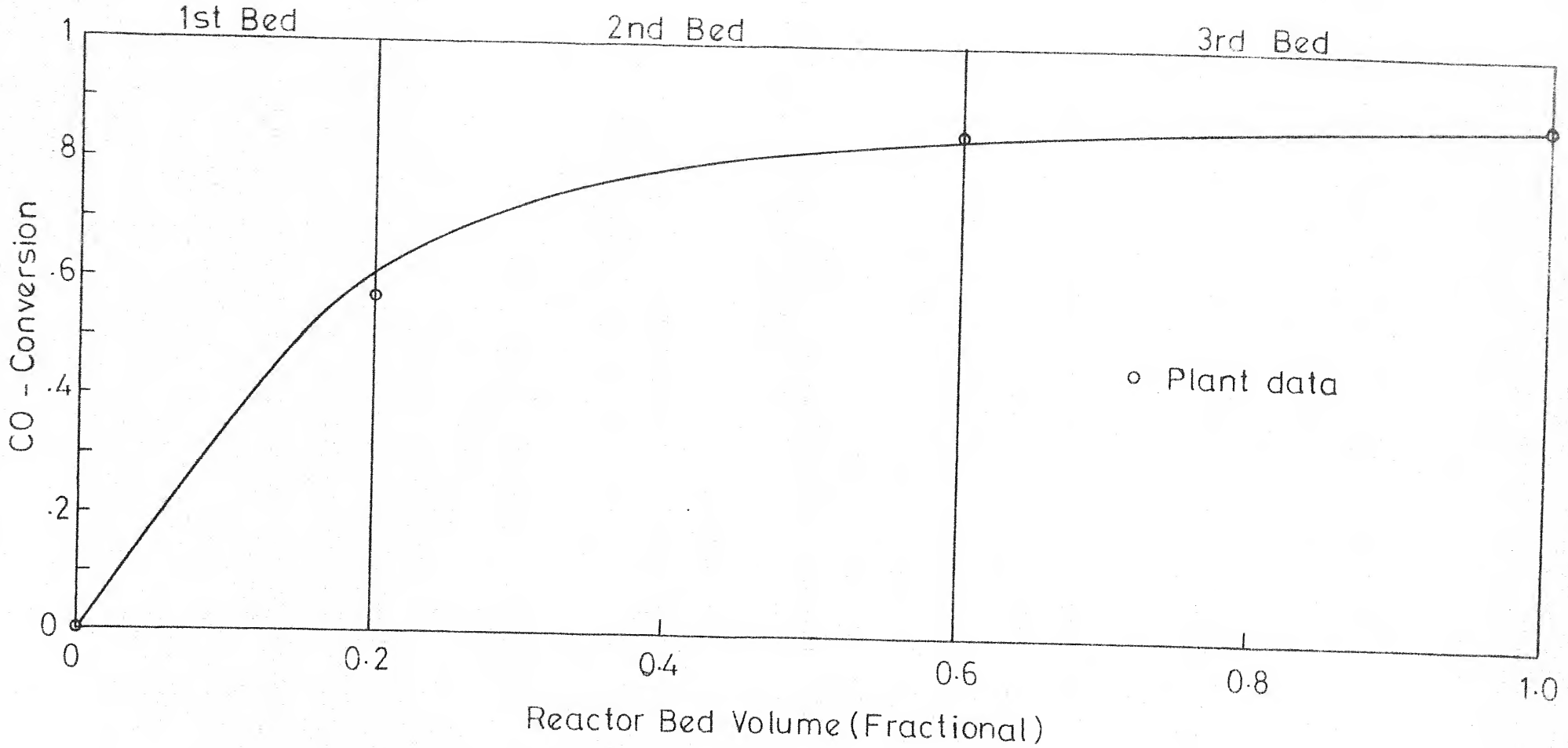

Fig. 4·5 - CO-Conversion profiles calculated in the reactor beds.

CHAPTER 5

OPTIMIZATION OF THE REACTOR

The simulation model formulated so far is used in an optimization scheme to achieve the maximum amount of reaction product from the existing multi-bed reactor. This is equivalent to maximizing the final extent of the reaction with a given feed state. For fixed amount of catalyst in each bed, this reduces to the determination of the inlet temperature, for each bed which will give the maximum final conversion of CO.

Thus the objective function, which is to be maximized, is the overall conversion of CO and this can be expressed by (Ref. Fig. 2.2):

$$\sum_{n=1}^{N} (x_{n,L} - x_{n,0}) = (x_{N,L} - x_{1,0}) \qquad (5.1)$$

Where

N = number of beds in the reactor

$x_{n,0}$ = degree of conversion at the inlet of bed n

$x_{n,L}$ = degree of conversion at the exit of bed n

The optimum temperature profiles over the reactor are to be determined subject to the following constraints.

i) A fixed volume of each bed gives

$$V_n = F \cdot y_{f,CO} \int_{x_{n,0}}^{x_{n,L}} \frac{dx}{r} \qquad n = 1,2,\ldots,N \quad (5.2)$$

ii) $T_{n,L} < T^*_{n,L}$ (5.3)

This represents the natural constraint on the bed exit temperature which must lie below the equilibrium temperature corresponding to the exit composition.

iii) In addition, the reactor temperature may be constrained below a maximum permissible value T_m, so that

$$T \leq T_m. \quad (5.3a)$$

For the present reactor, the temperature may be limited to 500°C[30] to prevent the deterioration of shift catalyst at higher temperatures. The temperature would exceed 500°C, if at all, only toward the end of the first bed. Therefore, the imposition of this temperature constraint may not be utilized in each and every case.

Optimization-Method

The solution of the optimization problem under consideration may be obtained either by a direct application of dynamic programming[37], or by using a direct search technique based on analytical criteria[38] for the optimal policy. The dynamic programming approach may involve considerable computation. The direct search approach, on the other hand, requires

numerical evaluation of the integral (Ref. Eqn.(2.6)) which involves the temperature derivative of the rate function. The experimental rate data must then be known with higher accuracy in order to find out this derivative.

In the present work, another technique[39] has therefore been used which is based on a combination of analytic criteria for the optimum and a dynamic programming formulation. This technique is based essentially on the dynamic programming approach but utilizes a simple numerical search routine for single-bed optimization and the rate matching criterion of eqn.(2.7) between two beds (n-1) and n. These search routines are described here briefly.

Single-bed Optimization

The optimal policy for a one-bed reactor with a fixed volume and given exit composition is determined using Modified Fibonacci search technique[40]. This amounts to a single variable search over reactor exit temperature within the specified range and finding the corresponding inlet conditions (by carrying out backward integration on the catalyst bed) in order to achieve the maximum conversion in the bed. The upper limit of the temperature range in which search is made is determined by the constraints represented by eqns. (5.3) and (5.3a) whereas a reasonable value for the lower limit is taken as 325°C. The equilibrium temperature to be used in eqn.(5.3)

may be calculated from eqns. (4.19),(4.20a) and (4.21) at the given composition.

Rate-Matching

If the temperature $T_{n,0}$ and stream composition $x_{n,0}$ at the inlet of bed n are known, the rate-match criterion of eqn.(2.7) can be applied between beds (n-1) and n to determine the temperature, $T_{(n-1),L}$ at the end of bed (n-1) at the same composition (Ref. eqn. (2.7a)). This is accomplished by using direct search over temperature. The procedure used for converging to the required temperature is as follows:

A trial value for the temperature $T_{(n-1),L}$ is selected which is higher than the temperature $T_{n,0}$ by some specified increment. The corresponding value of the reaction rate is calculated at the end of bed (n-1) and is compared with the value at the inlet of bed n. If the calculated value is higher, the process is continued using the same increment in temperature. On the other hand, if the calculated value is lower then the temperature has already passed through the desired point. At this stage the calculation is backed up by one trial and the process is repeated using a smaller increment until the temperature is determined within desired accuracy.

General Structure of the Algorithm

Starting from the outlet end of the reactor, last bed

is optimized first using the single-bed optimization routine with an assumed value of overall conversion $x_{N,L}$. The remaining beds are subsequently optimized by means of the rate-matching criterion. If at the inlet of first bed, the relation

$$x_{1,0} = 0 \qquad (5.4)$$

gets satisfied, the assumed value of $x_{N,L}$ is correct. Otherwise a new value is assumed (using a similar trial and error procedure as indicated for rate-matching) and the solution is repeated until eqn.(5.4) is satisfied within predetermined tolerances.

While optimizing the reactor by this method, the upper temperature constraint of eqn.(5.3a) has not been applied except for the last bed (for which single bed optimization method is used). As mentioned earlier in this chapter, the first bed exit temperature, $T_{1,L}$, may then exceed the permissible limit, T_m(= 500°C), in some of the cases which is not desireable. The imposition of the temperature constraint in such cases becomes necessary to avoid excessive temperature and this thus eliminates the use of rate-matching criterion between first and second bed.

In such a case, the problem is solved again (the actual of $x_{N,L}$ for this case must be very close to the one determined by the earlier method) by applying the earlier

method for optimization upto the second bed and then optimizing the first bed using single-bed optimization method which automatically takes care of the desired temperature constraint. An optimal N-stage policy is thus determined.

The computations have been done on IBM 7044 computer using Fortran IV language (the Program is presented in Appendix VI.).

***

CHAPTER 6

RESULTS AND DISCUSSION

1. The optimum conversion has been calculated for the existing feed composition and reactor load. Table 6.1 presents the results of computation for this case. The actual plant data are also included for comparison.

An increase of about 3% in conversion of CO from 87.97% to 91.14% can be achieved provided the inlet temperature to each stage is properly adjusted. These temperatures determined for the optimum reactor performance are, however, far from the existing ones.

2. For observing the effect of different variables on the performance of the reactor, several different sets with varying steam/gas ratio, dry gas feed rate and catalyst-age have been studied. In each case the overall conversion of CO has been optimized at the existing dry gas composition. Tables 6.2 to 6.4 show the values of these variables for the different sets and the resulting optimum conversions and temperatures.

2.1 Variation in Steam/Gas Ratio

a. Over the range studied, it can be observed from Table 6.2 that if the dry gas feed rate is maintained constant, the optimum CO conversion increases though the increase becomes less sharp with increasing steam/gas ratio.

TABLE 6.1

OPTIMUM REACTOR PERFORMANCE FOR EXISTING FEED COMPOSITION AND REACTOR LOAD

Catalyst age, days	Inlet steam/ gas ratio (volume)	Dry Gas Feed rate, $NM^3/hr.$	Bed No.	Computed Optimum Conditions					Plant Conditions			
				Temperature, °C					Temperature, °C			
				Inlet	Exit	Exit equilibrium	Overall CO conversion %	Overall H_2 production, $NM^3/hr.$	Inlet	Exit	Overall* CO Conversion,%	Overall* H_2 production $NM^3/hr.$
270	1.07	17830	1	343.73	498.96	524.84	77.51	15096	351	460	56.94	13607
			2	357.21	377.08	426.40	87.48	15818	400	459	84.14	15576
			3	333.65	340.90	384.22	91.14	16083	406	415	87.97	15853

*calculated from gas composition

This behaviour appears to be as a result of a more favourable equilibrium for the increased ratio but a decreased contact time because the total flow rate becomes higher when more steam is present. Thus beyond a certain limit, an increasing ratio is not much effective in improving the conversion as can be seen from Fig. 6.1.

b. The adiabatic temperature rise is lower in case of higher steam/gas ratio. This can be attributed to the fact that the heat of reaction is utilized in providing sensible heat to a larger volume of gas-steam mixture.

c. The sets of optimum inlet temperatures show a consistent pattern. The temperature to each stage becomes higher when a higher steam/gas ratio is used. The reason for this behaviour may be that the heat of reaction raises the temperature of the larger volume of gas-steam mixture to a lesser extent, thus decreasing the catalyst activity. This unfavourable effect can be compensated by using a higher inlet temperature.

2.2 Variation in Dry Gas Feed Rate

a. An increase in flow rate at a fixed steam/gas ratio leads to a decreased optimum CO-conversion (Table 6.3). This seems to be natural because a higher gas rate should retard the reaction due to a decrease in contact time. Moreover, it can be observed from Fig. 6.1 that the decrease in optimum conversion with dry gas feed rate is a linear one.

TABLE 6.2*

EFFECT OF STEAM/GAS RATIO

Set No.	Catalyst age, days	Inlet steam/ gas ratio (volume)	Dry gas feed rate, $NM^3/hr.$	Bed No.	Computed optimum conditions Temperature, °C Inlet	Exit	Exit-equilibrium	Overall CO conversion %	Overall H_2 production, $NM^3/hr.$
				1	330.28	498.96	527.77	68.52	14446
1.	270	0.75	17830	2	352.12	380.05	432.85	80.06	15281
				3	333.80	345.39	392.12	84.86	15628
				1	362.98	498.96	527.97	83.51	15531
2.	270	1.50	17830	2	365.03	378.11	425.82	91.61	16117
				3	335.30	339.62	382.26	94.31	16313
				1	382.38	498.96	537.34	86.93	15779
3.	270	2.00	17830	2	373.57	382.54	430.31	93.71	16269
				3	339.73	342.51	385.39	95.84	16423
				1	398.65	498.96	551.40	88.67	15904
4.	270	2.50	17830	2	382.43	389.26	438.12	94.76	16345
				3	345.83	347.85	391.05	96.58	16477

*The data at steam/gas ratio of 1.07 have already been given in Table 6.1.

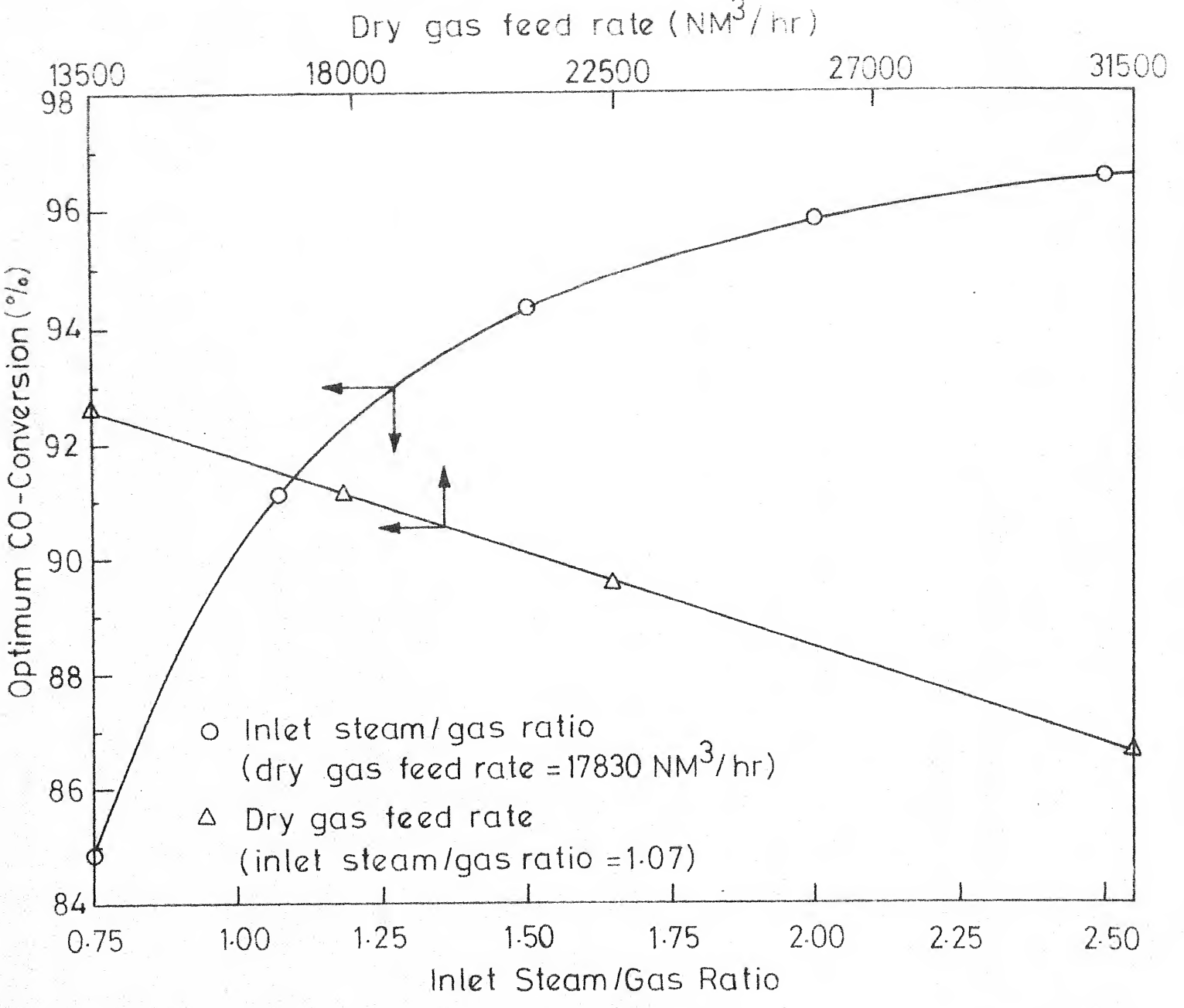

Fig.6·1 - Effect of Steam/Gas Ratio and Dry Gas Feed Rate.

b. The optimum inlet temperature is higher at the higher dry gas feed rate. The higher inlet temperature with an increased catalyst activity seems to compensate, in part, for the reduced degree of conversion.

2.3 Variation in Catalyst-Age

The effect of time of operation beyond a period of 270 days, has very little effect on either the optimum temperatures or on the conversion (Table 6.4). The optimum conversion is reduced by a negligible amount and the temperature variation is within 1° to 2°C only. However with passage of time, mechanical properties of catalyst pellets will deteriorate and necessitate replacement after about three years.

3. Finally after studying the effect of individual plant variables, a two-level factorial design has been used to study the effect of interaction between steam/gas ratio and dry gas feed rate at the existing composition of dry gas. The combinations of the variables with the resulting optimum conditions are shown in Table 6.5.

Experiments for this two level design have been carried out at conditions shown in Figure 6.2. The results are also included in the same figure. Following observations can be made.

a. Increase in steam/gas ratio increases CO conversion.

b. Increase in dry gas feed rate decreases CO conversion

TABLE 6.3*: EFFECT OF DRY GAS FEED RATE

Set No.	Catalyst age, days	Inlet steam/ gas Ratio (Volume)	Dry gas feed Rate, NM^3/hr.	Bed No.	Computed Optimum Conditions Temperature, °C Inlet	Exit	Exit-Equilibrium	Overall CO conversion %	Overall H_2 Production NM^3/hr
1	270	1.07	13500	1	320.29	480.16	499.64	80.15	11575
				2	340.83	359.32	404.53	89.45	12085
				3	319.32	325.68	364.29	92.67	12261
2.	270	1.07	22500	1	349.38	498.96	554.92	74.33	18760
				2	373.02	395.08	448.28	85.38	19770
				3	347.58	355.86	403.36	89.55	20150
3.	270	1.07	31500	1	362.00	498.96	616.64	67.95	25448
				2	399.07	426.09	486.56	81.50	27181
				3	371.40	381.64	435.19	86.64	27838

*The data at dry gas feed rate of 17830 NM^3/hr have already been given in Table 6.1.

TABLE 6.4*: EFFECT OF CATALYST-AGE

Set No.	Catalyst age, days	Inlet steam/ gas Ratio (volume)	Dry Gas Feed Rate, $NM^3/hr.$	Bed No.	Computed Optimum Conditions – Temperature, °C Inlet	Exit	Exit equili-brium	Overal CO Conversion %	Overall H_2 Production $NM^3/hr.$
				1	345.68	498.96	526.21	77.36	15086
1	450	1.07	17830	2	358.69	378.58	427.97	87.34	15808
				3	334.83	342.13	385.78	91.02	16074
				1	345.49	498.96	527.97	77.18	15073
2	630	1.07	17830	2	359.66	379.67	429.14	87.22	15799
				3	335.61	342.96	386.95	90.92	16068
				1	344.62	498.96	529.53	77.00	15059
3	810	1.07	17830	2	360.25	380.41	430.31	87.11	15791
				3	336.66	344.08	387.93	90.85	16062

*The data for catalyst-age of 270 days have already been given in Table 6.1

c. The effect of interaction of above two variables is marginal because the effect of one is offset by the effect of the other.

4. In almost all the cases studied in this investigation, it has been observed that the exit temperature from the first bed is always very close to maximum permissible temperature of 500°C. Moreover the optimum exit temperature from the last bed occurs within 36 to 52°C of the corresponding equilibrium temperature.

TABLE 6.5: EFFECT OF INTERACTION BETWEEN STEAM/GAS RATIO AND DRY GAS FEED RATE

Set No.	Catalyst age, days	Inlet steam/gas Ratio (Volume)	Dry Gas Feed Rate, $NM^3/hr.$	Bed No.	Computed Optimum Conditions				
					Temperature, °C			Overall CO conversion %	Overall H_2 production $NM^3/hr.$
					Inlet	Exit	Exit equilibrium		
1	270	2.00	31500	1	396.02	498.96	671.72	76.71	26569
				2	428.25	444.84	504.72	89.22	28168
				3	387.34	392.27	444.76	92.93	28643
2	270	1.50	22500	1	368.68	498.96	562.14	80.51	19324
				2	382.13	397.37	449.45	89.93	20185
				3	351.43	356.58	402.57	93.12	20477
3	270	1.50	13500	1	340.98	481.76	501.40	85.80	11884
				2	346.18	357.91	402.97	93.09	12284
				3	321.97	325.63	361.75	95.39	12410

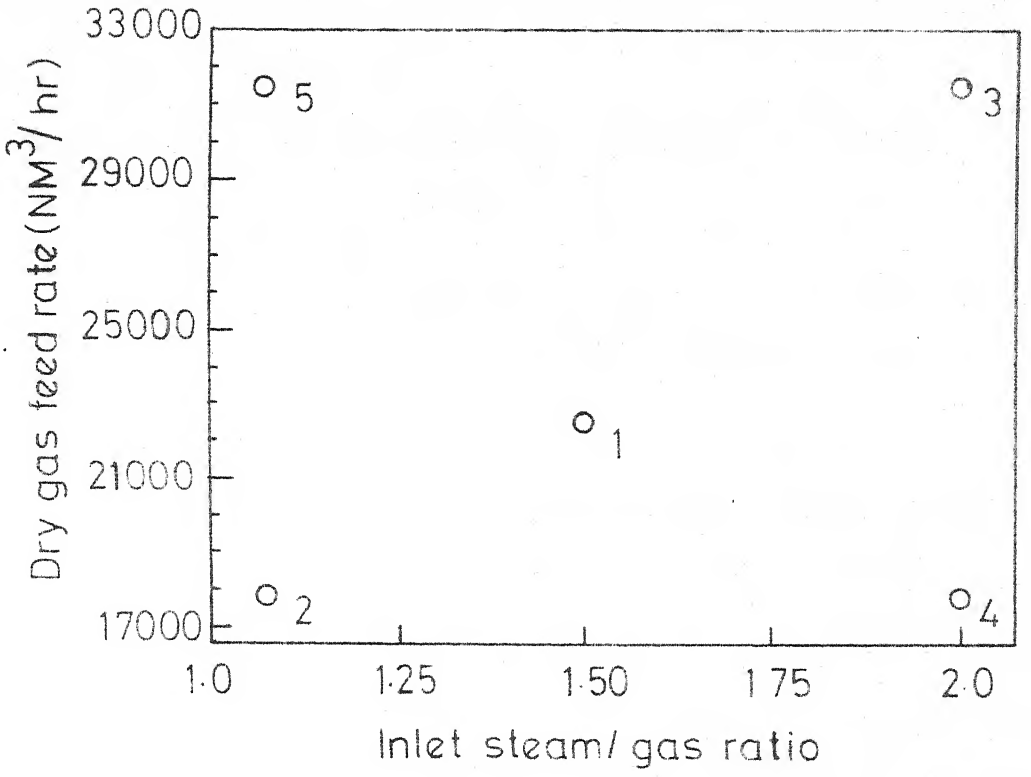

Response	% CO-Conversion (X)
Object	Maximization
Calculated values	86·64 92·93 93·12 91·14 95·84
Ratio effect	$(X_3 + X_4 - X_2 - X_5)/2 = 5{\cdot}50$
Gas feed effect	$(X_3 + X_5 - X_2 - X_4)/2 = -3{\cdot}70$
Ratio x Gas feed interaction effect	$(X_2 + X_3 - X_4 - X_5)/2 = 0{\cdot}80$

Fig. 6·2 - Calculated 'Effects' of the variables.

CHAPTER 7

CONCLUSIONS AND SUGGESTIONS

A mathematical model has been developed for a shift reactor which simulates the plant performance with reasonable accuracy. The results of optimization indicate that the conversion of the reactor studied can be improved by about 3% by appropriately altering the temperatures. A further scope for improvement exists in principle by the use of a higher steam/gas ratio. These changes must, however, be supported with the financial and operating aspects of the plant, particularly, when the optimization of the entire shift conversion loop is desired. In that case the optimization has to be performed based on a plant profit function which includes heat recovery and steam separation costs together with capacity limitation on various units.

The optimization-results obtained in this investigation will serve as a guide and a valuable starting point for optimizing the entire plant.

***

APPENDIX I

CONDITIONS FOR OPTIMIZATION OF MULTIBED ADIABATIC REACTOR

The problem of finding minimum holding time to achieve a certain conversion is equivalent to that of determining the maximum conversion obtainable with a fixed holding time in a given number of sections[3]. The two problems are duals of one another and the solution to both of these is the same.

The holding time of bed n (Ref. Fig. 2.2) in a multistage sequence can be written as

$$\theta_n = \int_{y_{n,o}}^{y_{n,L}} \frac{dy}{r} \qquad (I.1)$$

with

$$r = r\,(y,T).$$

here,

θ = reactor holding time

y = mole fraction of product.

For an N-stage system, the total holding time, θ_T, becomes

$$\theta_T = \sum_{1}^{N} \theta_n = \sum_{1}^{N} \int_{y_{n,o}}^{y_{n,L}} \frac{dy}{r} \qquad (I.2)$$

For the minimization of the total holding time for the sequence, it is possible to use analytical techniques to obtain

direct criteria for the optimal policy. The development shown below follows from the work done originally by HORN[38]. The approach is illustrated for a two-stage sequence for the sake of convenience. The function to be minimized may be written as from eqn.(I.2).

$$\theta_T = \int_{y_{1,o}}^{y_{1,L}} \frac{dy}{r} + \int_{y_{2,o}}^{y_{2,L}} \frac{dy}{r} \qquad (I.3)$$

Since there is no reaction in the interchanger,

$$y_{1,L} = y_{2,o}$$

If $y_{1,o}$ and $y_{2,L}$ are considered known, then

$$\theta_T = \theta_T (T_{1,o};\ y_{1,L};\ T_{2,o}) \qquad (I.4)$$

The necessary conditions for θ_T to be minimized are found from the calculus.

$$\left(\frac{\partial \theta_T}{\partial T_{1,o}}\right)_{y_{1,L};T_{2,o}} = \left(\frac{\partial \theta_T}{\partial y_{1,L}}\right)_{T_{1,o};T_{2,o}}$$

$$= \left(\frac{\partial \theta_T}{\partial T_{2,o}}\right)_{T_{1,o};\ y_{1,L}} = 0 \qquad (I.5)$$

On applying these conditions the following results.

$$\left[\frac{\partial \theta_T}{\partial T_{1,o}}\right]_{y_{1,L};T_{2,o}} = \int_{y_{1,o}}^{y_{1,L}} \frac{1}{r^2} \cdot \frac{\partial r}{\partial T} \cdot dy = 0 \qquad (I.6)$$

Similarly,

$$\left[\frac{\partial \theta_T}{\partial T_{2,0}}\right]_{y_{1,L};T_{1,0}} = \int_{y_{2,0}}^{y_{2,L}} \frac{1}{r^2} \cdot \frac{\partial r}{\partial T} \cdot dy = 0 \qquad \text{(I.7)}$$

Finally,

$$\left[\frac{\partial \theta_T}{\partial y_{1,L}}\right]_{T_{1,0};T_{2,0}} = \frac{1}{r(y_{1,L};\ T_{1,L})} - \frac{1}{r(y_{2,0};T_{2,0})} \qquad \text{(I.8)}$$

$$= 0$$

$$\therefore \quad r(y_{1,L};\ T_{1,L}) = r(y_{2,0};\ T_{2,0}) \qquad \text{(I.9)}$$

The optimal policy must therefore satisfy the criteria represented by equations (I.6), (I.7) and (I.9). This approach may be extended to the case of an N-bed sequence with the following results:

$$\int_{y_{n,0}}^{y_{n,L}} \frac{1}{r^2} \cdot \frac{\partial r}{\partial T} \cdot dy = 0$$

$$n = 1,2,\ldots,N \qquad \text{(I.10)}$$

and

$$r(y_{n-1,L};\ T_{n-1,L}) = r(y_{n,0};\ T_{n,0}) \qquad n = 2,3,\ldots,N \qquad \text{(I.11)}$$

which may be written as

$$r_{(n-1),L} = r_{n,0} \qquad n = 2,3,\ldots,N \qquad \text{(I.11A)}$$

APPENDIX II

A. Effect of Pressure on Specific Heat

From the specific heat data of Joseph[24] for various gases, it has been found that the pressure dependency for gases H_2, CO, CO_2, CH_4, N_2 and A is negligible upto 40 atms. but in case of steam it is significant. The pressure-dependency has, therefore, been taken into account only in the case of steam.

Table II.1 lists the specific heat data[24] for steam in the pressure range of 1 to 40 atm.

TABLE II.1: SPECIFIC HEAT OF STEAM

Temperature °K	Specific Heat, C_p/R			
	1 atm.	10 atm.	20 atm.	40 atm.
550	4.335	4.708	5.260	6.967
600	4.391	4.618	4.921	5.723
700	4.522	4.627	4.754	5.043
800	4.665	4.724	4.792	4.937

On a logarithmic plot of $(\frac{C_p - C_{p_o}}{R})$ against P or T, straight lines are obtained as shown in Fig. II.1 and II.2. The value $(C_p - C_{p_o})$ is the difference of the specific heats in the real state and the ideal state (P=1 atm.). Thus, for steam an equation of the form

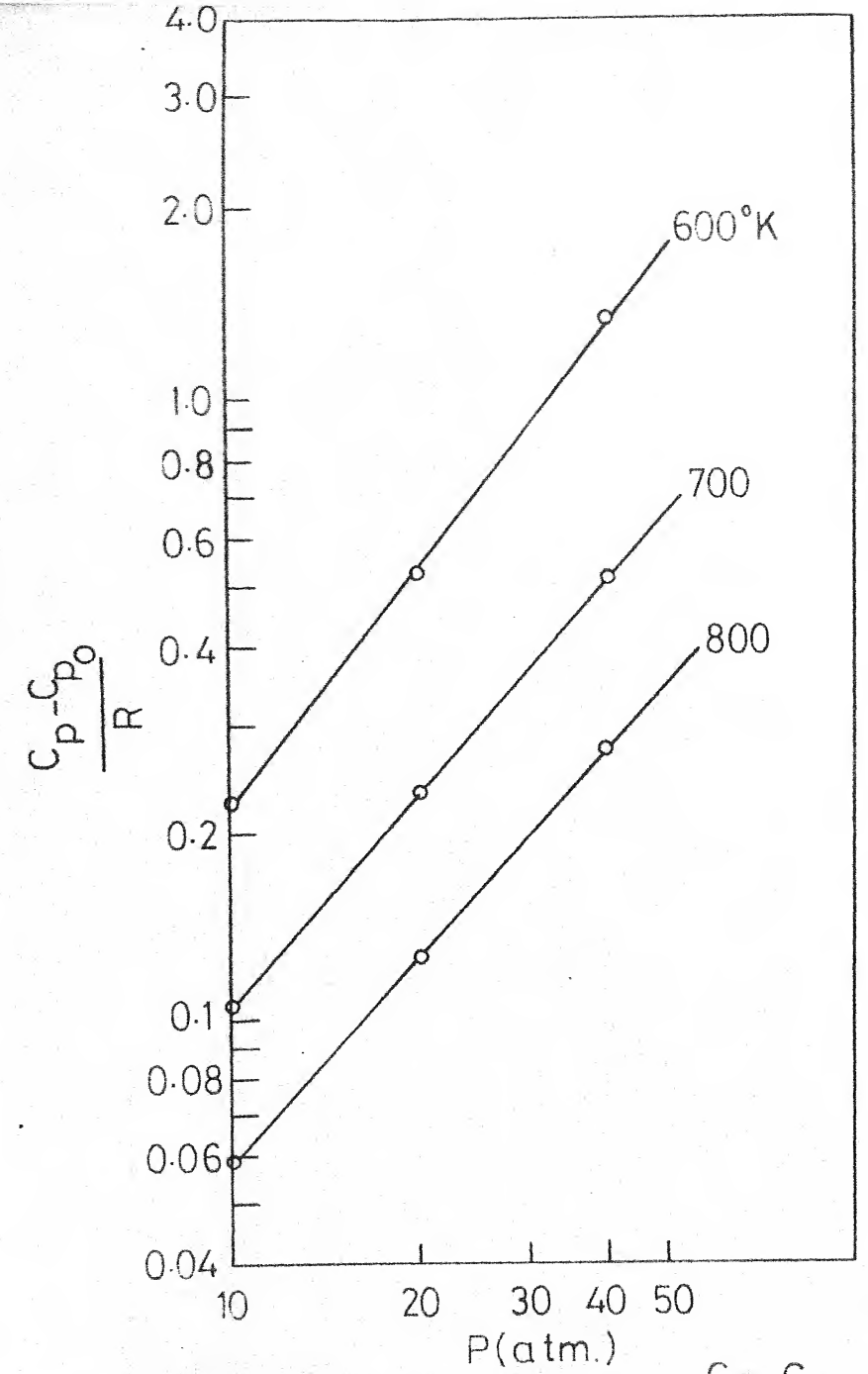

Fig. II-1 -Logarithmic plot of $\left(\frac{C_p-C_{p_o}}{R}\right)$ vs. Pressure for Steam.

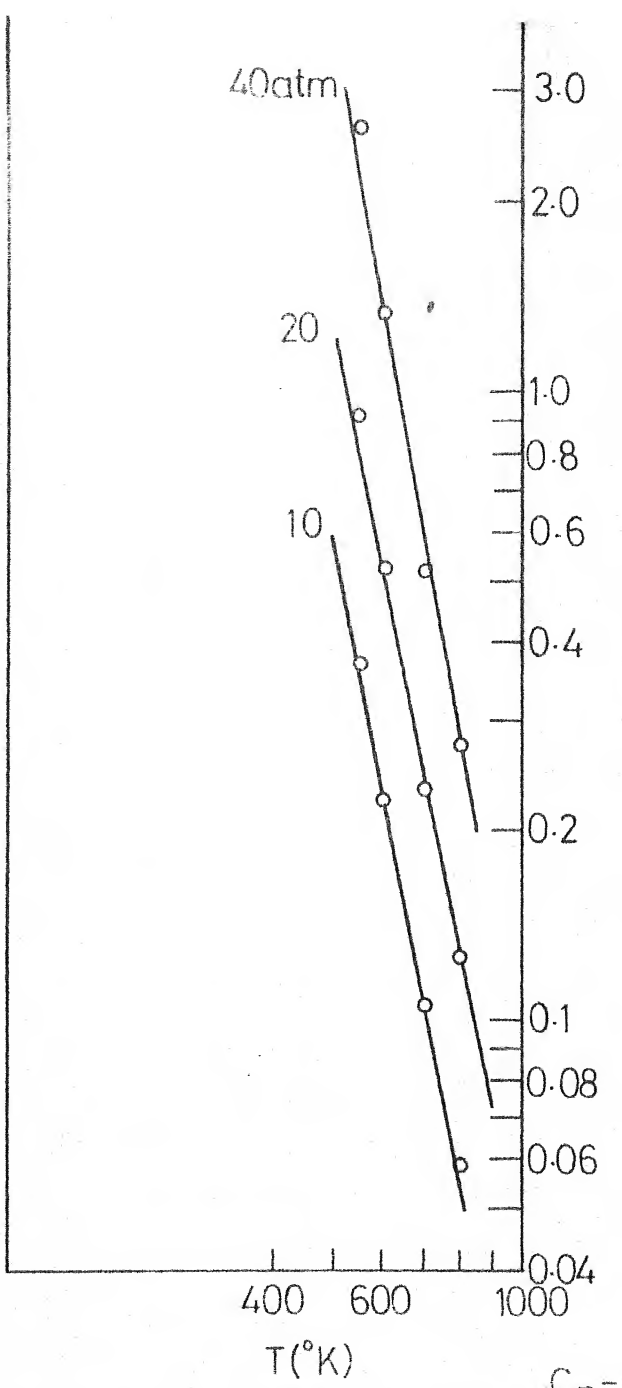

Fig. II-2 -Logarithmic plot of $\left(\frac{C_p-C_{p_o}}{R}\right)$ vs. Temperature for Steam

$$(C_p - C_{p_o}) = U\, T^V\, P^W \qquad \text{(II.1)}$$

is valid and the following values have been evaluated for the constants U, V and W.

$U = 0.63 * 10^{14}$

$V = -5.56$

$W = 1.29$

The above equation is applicable at least in the temperature range of 600 to 800°K and for pressures upto 40 atm.

B. Effect of Temperature and Pressure on Heat of Reaction

The standard heat of reaction at 25°C and 1 atm. pressure may be calculated from the heat of formation data[23] of Table II.2 by means of the equation:

$$\Delta H^o_R = \sum \Delta H^o_{f(\text{products})} - \sum \Delta H^o_{f(\text{reactants})} \qquad \text{(II.2)}$$

TABLE II.2: STANDARD HEATS OF FORMATION

(Conditions: 25°C, 1 atm. pressure, gaseous substances)

Compound	Standard Heat of Formation, g-cal/g.mole ΔH^o_f
$H_2(g)$	0
$CO(g)$	-26,415.7
$CO_2(g)$	-94,051.8
$H_2O(g)$	-57,797.9

For the reaction

$$CO\ (g) + H_2O\ (g) \longrightarrow CO_2(g) + H_2\ (g)$$

the standard heat of reaction is calculated by means of eqn.(II.2):

$$\Delta H_R^o = (-94,051.8) + 0 - (-26,415.7) - (-57,797.9)$$
$$= -9,838 \text{ cal/gmmole}$$

Taking 600°K and 1 atm. pressure as the reference state (this corresponds to lower range of normal operating conditions for H.T. shift reaction), the following equation may be applied for determining the effect of temperature on the Heat of Reaction at constant pressure[35]:

$$\Delta H_R(T,P) = \Delta H_R(T_o,P) + \int_{T_o}^{T} \Delta C_p \, dT \qquad \text{(II.3)}$$

where ΔC_p = change in heat capacity of entire system at constant pressure.

$$= (C_p)_{\text{products}} - (C_p)_{\text{reactants}}$$

∴ The heat of reaction at 600°K and 1 atm pressure is

$$\Delta H_R(600°K,\ 1 \text{ atm.}) = \Delta H_R^o + \int_{T_o=298}^{T=600} \Delta C_p \, dT \qquad \text{(II.3a)}$$

At atmospheric pressure, the gas is ideal and the molal heat capacities may be represented by an empirical equation of the form

$$C_p = a + bT + cT^2 \qquad \text{(II.4)}$$

Then,

$$\Delta C_p = \Delta a + \Delta bT + \Delta cT^2 \qquad \text{(II.5)}$$

Using eqn.(II.3a), the integration yields

$$\Delta H_R(600°K,\ 1\ atm.) = \Delta H_R^o + \left[\Delta a(T-T_o) + \frac{\Delta b}{2}(T^2-T_o^2) + \frac{\Delta c}{3}(T^3-T_o^3)\right] \qquad (II.3b)$$

in which $T_o = 298°K$

$T = 600°K$

$\Delta H_R^o = -9838$ cal/gm mole.

Using the values of empirical constants from Table 4.1,

$$\Delta a = a_{CO_2} + a_{H_2} - a_{CO} - a_{H_2O} = -0.201$$

$$\Delta b = b_{CO_2} + b_{H_2} - b_{CO} - b_{H_2O} = 5.493 * 10^{-3}$$

$$\Delta c = c_{CO_2} + c_{H_2} - c_{CO} - c_{H_2O} = -2.7177 * 10^{-6}$$

Substituting these values in eqn.(II.3b), the heat of reaction at the reference state (600°K, 1 atm.) is calculated to be

$$\Delta H_R\ (600°K,\ 1\ atm.) = -9328\ Cal/gmmole.$$

To evaluate the effect of pressure on heat of reaction at a constant temperature of 600°K, the principle that the enthalpy is a point function results in the equation[23]:

$$\Delta H_R(T,P) = \Delta H_R(T,\ 1\ atm) + \left[H_P(T,P) - H_P(T,\ 1\ atm)\right] - \left[H_R(T,P) - H_R(T,\ 1\ atm)\right] \qquad (II.6)$$

where H is the enthalpy and subscripts R and P refer to reactants and products, respectively.

Use of Eqn.(II.6) for the shift reaction then gives

$$\Delta H_R(T,P) = \Delta H_R(T,\ 1\ atm) + \left[H_{CO_2}(T,P) + H_{H_2}(T,P) - H_{CO_2}(T,1atm) - H_{H_2}(T,1atm)\right] - \left[H_{CO}(T,P) + H_{H_2O}(T,P) - H_{CO}(T,1atm) - H_{H_2O}(T,1atm)\right] \qquad (II.6a)$$

For the gaseous reactants and products, the enthalpy change in shifting from the lower to the higher pressure is evaluated using the data[24] given in Table II.3.

TABLE II.3: ENTHALPY OF REACTANTS AND PRODUCTS AT 600°K

Pressure atm.	Enthalpy at 600°K, $(H-E_o)/RT_o$			
	CO	$H_2O(g)$	CO_2	H_2
1	7.7546	8.965	9.802	7.6084
10	7.7528	8.811	9.764	7.6147
40	7.7486	8.216	9.635	7.6359

E_o = The zero reference point of the enthalpy, taken as the internal energy of the ideal gas at absolute zero.

R = 1.987 Cal/mole °K

T_o = 273.16°K

A plot of $-\Delta H_R$(600°K, P atm.) against P(in atm) on a semilog graph gives a straight line. The relation obtained for the variation of ΔH_R with pressure at 600°K is

$$\Delta H_R(600°K, P \text{ atm}) = -(0.933 * 10^4) \exp(-0.9354 * 10^{-3} P) \quad (II.7)$$

To evaluate the heat of reaction at any temperature and pressure in the normal operating range (600° - 800°K, 1-40 atm.), Eqn.(II.3) may be used with T_o = 600°K. The value of ΔH_R

(600°K, P atm.) may be substituted from eqn.(II.7). The value of ΔC_p above atmospheric pressure may be determined from the following eqn.

$$\Delta C_p = \Delta a + \Delta b.T + \Delta c.T^2 - UP^W T^V \quad (II.8)$$

TABLE II.4: CALCULATED VARIATION OF ENTHALPY DEPARTURE AND HEAT OF REACTION WITH PRESSURE (TEMPERATURE 600°K)

Pressure, P atm.	Enthalpy Departure at 600°K, cal/mole $\Delta H(600°K, P \text{ atm.}) = H(600°K, P \text{ atm}) - H(600°K, 1 \text{ atm})$				Heat of Reaction at 600°K and P atm. Pressure, $\Delta H_R(600°K, P \text{ atm})$ cal/gmmole
	CO	$H_2O(g)$	CO_2	H_2	
1	0	0	0	0	-9328
10	-0.978	-83.600	-20.64	3.424	-9260.64
40	-3.260	-407.000	-90.700	14.94	-8993.5

The final expression obtained after evaluating the integral term in eqn.(II.3) is given by

$$\Delta H_R(T,P) = \Delta H_R(600°K,P) + \left[\Delta a.T + \frac{\Delta b}{2}.T^2 + \frac{\Delta c}{3}.T^3 - c_2 P^W T^{V+1}\right] + c_3 P^{W-c_1} \quad (II.9)$$

with

$$c_1 = 672.47$$

$$c_2 = -13.82 * 10^{12}$$

$$c_3 = -2.96$$

APPENDIX III

DERIVATION OF THE PSEUDO-FIRST ORDER RATE EXPRESSION

For determining the reaction rate of CO conversion, the second order expression may be used for the reversible reaction

$$CO + H_2O\ (g) \underset{k_2'}{\overset{k_2}{\rightleftharpoons}} CO_2 + H_2$$

The overall rate of reaction can be expressed as:

$$r = k_2\, y_{CO}\, y_{H_2O} - k_2'\, y_{CO_2} \cdot y_{H_2} \qquad (III.1)$$

where;

k_2, k_2' = second order rate constants for the forward and the backward reaction respectively.

Since catalysis does not change the equilibrium but only increases the reaction rate in both directions, the relation, $K = k_2/k_2'$, between the rate constants and the equilibrium constant is valid also for the heterogeneous reaction.

Equilibrium constant K is related to the equilibrium composition by:

$$K = \frac{y^*_{CO_2} \times y^*_{H_2}}{y^*_{CO} \times y^*_{H_2O}} \qquad (III.2)$$

Substituting $k_2' = k_2/K$ in eqn.(III.1), we have

$$r = k_2 \left[y_{CO} \cdot y_{H_2O} - \frac{y_{CO_2}\, y_{H_2}}{K} \right] \qquad (III.3)$$

Combining with eqn.(III.2)

$$r = k_2 \left[y_{CO} \cdot y_{H_2O} - \frac{y_{CO_2}}{y^*_{CO_2}} \cdot \frac{y_{H_2}}{y^*_{H_2}} \cdot y^*_{H_2O} \cdot y^*_{CO} \right] \qquad \text{(III.4)}$$

Since $H_2O(g)$ is present in large excess, its concentration may be assumed to remain constant and equal to the mean value $\bar{y}_{H_2O}$.

The eqn.(III.4) then becomes

$$r = k_2 \, \bar{y}_{H_2O} \left[y_{CO} - b \, y^*_{CO} \right] \qquad \text{(III.5)}$$

with $$b = \frac{y_{CO_2}}{y^*_{CO_2}} \cdot \frac{y_{H_2}}{y^*_{H_2}} \cdot \frac{y^*_{H_2O}}{y_{H_2O}} < 1$$

The more the reaction approached equilibrium, the more b approaches unity, and it would become equal to one only for the equilibrium state. The equilibrium concentration, y^*_{CO}, for this reaction is only a small fraction of the original CO concentration in the inlet raw gas-steam mixture so that the error of taking b=1 would be negligible in the initial as well as in the final stage of the conversion.

Putting b=1, the final expression for the rate of reaction then becomes:

$$r = k_1 (y_{CO} - y^*_{CO}) \qquad \text{(III.6)}$$

with $k_1 = k_2 \, \bar{y}_{H_2O}$

Equation (III.6) is a pseudo first order rate equation in CO and k_1 may be termed the "pseudo first order rate constant" which depends, naturally, on the actual concentration of $H_2O(g)$.

APPENDIX IV

MISCELLANEOUS RELEVANT DATA

TABLE IV.1: SULFUR FACTOR DATA[33]

Concentration of H_2S in the gas (dry basis) ppm	Sulfur factor, f_s
0	1.000
60	0.650
100	0.575
150	0.525
200	0.490
250	0.460
300	0.440
350	0.419
400	0.400
450	0.390
500	0.380
1000	0.299
2000	0.239

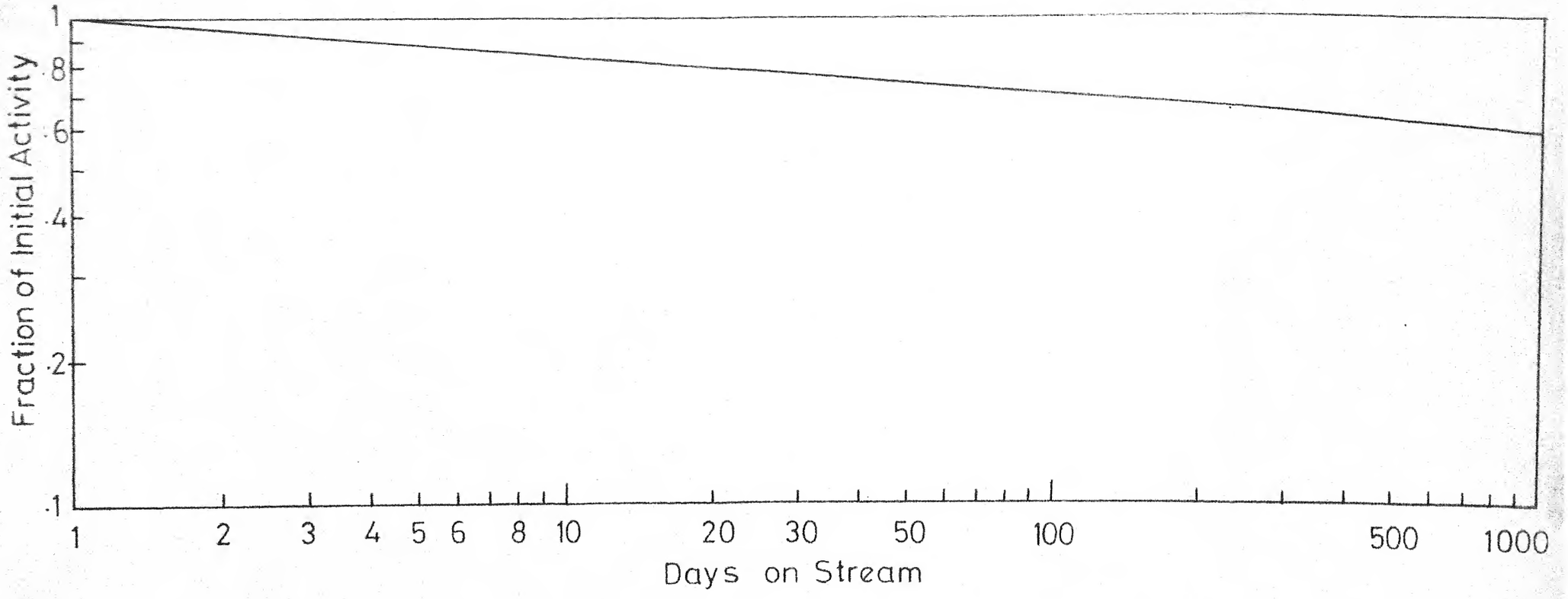

Fig.IV-1 - Effect of time of operation on Catalyst activity.

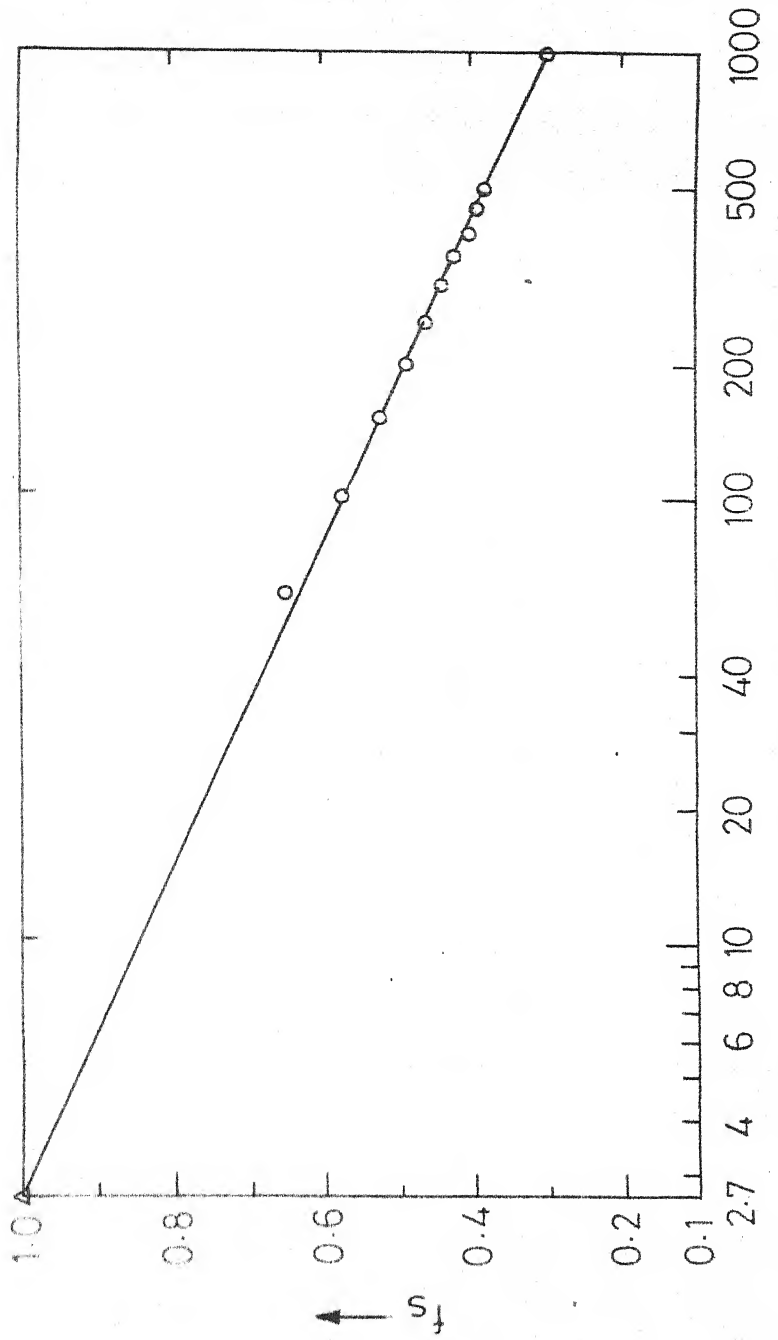

Fig. IV.2 – Plot of Sulfur factor vs. log (H_2S).

TABLE IV.2: CATALYST EFFECTIVENESS FACTOR CALCULATED ALONG THE LENGTH OF THE REACTOR BED*

Fractional bed length	Temperature, °K	Effectiveness factor
0	624.16	0.2673
0.1	637.31	0.2364
0.2	651.13	0.2085
0.3	665.35	0.1840
0.4	679.65	0.1630
0.5	693.66	0.1453
0.6	706.97	0.1308
0.7	719.27	0.1190
0.8	730.30	0.1097
0.9	739.95	0.1023
1.0	748.18	0.0965

*1st bed with the feed conditions as given in Table IV.3.

TABLE IV.3: PLANT DATA FOR THE SHIFT REACTOR

I. Catalyst

Type: FCI H.T. shift catalyst

Catalyst size and shape: 6 mm * 6 mm. cylindrical pellets

Age of the catalyst: 270 days

II. Reactor

No. of beds: 3

Reactor bed dia.: 9'6" (I.D.)

Catalyst distribution:

1st bed: 154 cuft.

2nd bed: 308 "

3rd bed: 308 "

III. Operating Conditions

Reactor Feed composition:-

H_2	53.2%
CO	40.6%
CO_2	3.2%
CH_4	0.4%
N_2 + A	2.6%
H_2S	40-50 ppm

Inlet steam/gas ratio (volume): 1.07

Inlet dry gas flow rate: 17830 NM^3/hr

Operating Pressure: 29.0 Kg/cm^2

	1st bed	2nd bed	3rd bed
Exit-gas Composition (%)			
H_2	59.6	63.1	64.6
CO	14.2	4.8	3.6
CO_2	23.0	29.4	30.0
$N_2 + CH_4 + A$	3.2	2.7	1.8
Temperature, °C (In/Out)	351/460	400/459	406/415

APPENDIX V

EQUILIBRIUM CONSTANT FOR WATER GAS SHIFT REACTION

The relationship between the standard free-energy change ΔF° and the equilibrium constant K is given by the expression:

$$\Delta F^\circ = - RT \ln K \qquad (V.1)$$

The value of ΔF° can be determined from the expression

$$\Delta F^\circ = \Delta H^\circ - T \Delta S^\circ \qquad (V.2)$$

where

ΔH° = Standard heat of reaction

ΔS° = Standard entropy change for the reaction.

The value of ΔH° is evaluated from the data for standard heats of formation (Table II.2):

$$\Delta H^\circ \ (298^\circ K) = (-94052 + 0) - (-26416 - 57798)$$

$$= - 9838 \text{ cal/gmmole}$$

and the ΔS° is evaluated from the Entropy data of Lavrov[34] given in Table V.1.

TABLE V.1: STANDARD VALUES OF ENTROPY
(Reference temperature = 25°C)

Compound	S° cal/mole °C
$CO_2(g)$	51.069
H_2 (g)	31.2110
CO (g)	47.216
$H_2O(g)$	45.106

Thus

$$\Delta S^{\circ}\ (298^{\circ}K) = (51.069 + 31.211) - (47.216 + 45.106)$$
$$= -10.042 \quad \text{cal/(gmmole)(°C)}$$

The temperature dependence of equilibrium constant can be determined using the data for heat capacities (Table 4.1) of reacting substances with the following equations:

$$\Delta H^{\circ}(T) = \Delta H^{\circ}(T_o) + \int_{T_o}^{T} \Delta C_p \, dT \qquad \text{(II.3a)}$$

and

$$\Delta S^{\circ}(T) = \Delta S^{\circ}(T_o) + \int_{T_o}^{T} \frac{\Delta C_p}{T} \, dT \qquad \text{(V.3)}$$

The quantity ΔC_p is given by equation (II.5) and from this

$$\int_{T_o=298^{\circ}K}^{T} \Delta C_p \, dT = \Delta a.T + \frac{\Delta b}{2} .T^2 + \frac{\Delta c}{3} . T^3 - 160.220$$

$$\int_{T_o=298^{\circ}K}^{T} \frac{\Delta C_p}{T} \, dT = \Delta a. \ln T + \Delta b.T + \frac{\Delta c}{2} . T^2 - 0.372$$

Substituting these values and combining eqns.(V.2), (V.3) and (II.3a), the final expression obtained for ΔF° is

$$\Delta F^{\circ}(T) = - 9998.220 + (\Delta a + 10.414)T$$
$$- \frac{\Delta b}{2} . T^2 - \frac{\Delta c}{6} . T^3 - \Delta a.T. \ln T \qquad \text{(V.4)}$$

and inserting this in eqn.(V.1) gives

$$\ln K = \left(\frac{1}{-RT}\right) \left[-9998.220 + (\Delta a + 10.414)\ T\right.$$
$$\left. - \frac{\Delta b}{2} T^2 - \frac{\Delta c}{6} .T^3 - \Delta a.T.\ln T\right] \qquad \text{(V.5)}$$

APPENDIX VI

COMPUTER - PROGRAMME

for

OPTIMIZATION OF REACTOR

```
C * * * * * * * * * * * * * * * * * * * * * * * * * * * * * * * * * * * * * * *
C
C                                OPTIMIZATION-PROGRAM
C
C * * * * * * * * * * * * * * * * * * * * * * * * * * * * * * * * * * * * * * *
C
C***  SIMULATION OPTIMISATION OF WATER GAS SHIFT REACTOR
C***  OPTIMISATION TO GET MAX.DEGREE OF CONVERSION IN MULTIBED ADIABATIC
C***  REACTOR.THE NO.OF BEDS AND VOLUME OF EACH BED IS SPECIFIED.
C***  MATERIAL-ENERGY BALANCE EQNS.(TWO FIRST ORDER SIMULTANEOUS
C***  DIFFERENTIAL EQNS.) ARE SOLVED USING RUNGE-KUTTA METHOD.
C***  RATE EQN. IS PSEUDO FIRST ORDER OBTAINED BY SIMPLIFYING
C***  SECOND ORDER RATE EXPRESSION(LAUPICHLER,MOE)
C***  FOR FCI H.T.SHIFT CATALYST(CHANDRAS PILOT PLANT DATA).
C-*-  NOTATION FOR INPUT DATA
C-*-  PERC(NC)=INLET GAS COMPOSITION(VOLUME PERCENT DRY BASIS)
C-*-  COMPONENT NO.AND NAME IS AS GIVEN -----------
C-*-  1=H2,     2=CO,     3=CO2,     4=CH4,     5=N2,     6=A,       7=H2O
C-*-  FDGS(1)=INLET DRY GAS FLOW ,      RSG(1)=STEAM/GAS RATIO INLET
C-*-  P=PRESSURE,         DP=CATALYST SIZE
C***  UNITS-- TIMDAY=TIME IN DAYS(ON STREAM)---(GREATER THAN 1 DAY)
C***  UNITS-- H2SPPM=CONCN.OF H2S IN PPM.(DRY BASIS)
C***  P=KG/CM2 ABS
C***  DP=PARTICLE DIA=CM.
C * * * * * * * * * * * * * * * * * * * * * * * * * * * * * * * * * * * * * * *
      DIMENSION PERC(100),FC(100),CONV(10),FDGS(25),RSG(25),FTS(25)
      DIMENSION YCONV(10),YF(10),Y(100),TCS(25),X(25),VOLUME(10)
      DIMENSION XEOPTM(10),TIOPTM(10),TEOPTM(10),TEEQLM(10)
      DIMENSION XE(10),TE(10),XI(10),TI(10),RATI(10),XIOPTM(10)
      DIMENSION ACP( 7),BCP( 7),CCP( 7)
      TKO=273.16
      NCOMP=7
      NS=1
      NC1=1
      NC2=NC1+1
      NC6=NC1+5
      NC7=NC1+6
      DATA ACP/6.946,6.350,6.339,3.204,6.457,4.97,7.136/
      DATA BCP/-0.196E-3,1.811E-3,10.14E-3,18.41E-3,1.389E-3,0.,2.64E-3/
      DATA CCP/0.4757E-6,-0.2675E-6,-3.415E-6,-4.48E-6,-0.069E-6,0.0,
     10.0459E-6/
      READ 146,P,DP,NBED
  146 FORMAT(2F11.2,I11)
      READ 143,(PERC(NC),NC=NC1,NC6)
  143 FORMAT(6F11.2)
      READ 144,FDGS(NS),RSG(NS)
  144 FORMAT(2F11.2)
      READ 145,(VOLUME(NB),NB=1,NBED)
  145 FORMAT(3F11.3)
      READ 147,H2SPPM,TIMDAY
```

```
  147 FORMAT(2F11.1)
      READ 148,TIMINT,NTIMEL
  148 FORMAT(F11.1,I11)
      PRINT 445
C * - * - * - * - * - * - * - * - * - * - * - * - * - * - * - * - * - * - * - * - * - * - *
      PRINT 455
      PRINT 999
  999 FORMAT(/4X,*OPTIMIZATION OF TROMBAY SHIFT REACTOR ---AT DIFFERENT
     1COMBINATIONS OF STEAM/GAS RATIO AND DRY GAS FLOW*/)
      PRINT 455
C * - * - * - * - * - * - * - * - * - * - * - * - * - * - * - * - * - * - * - * - * - * - *
      PRINT 150
  150 FORMAT(//4X,*INPUT DATA*)
      PRINT 156,(PERC(NC),NC=NC1,NC6)
  156 FORMAT(4X,*PERC(NC)*,5X,6F13.2)
      PRINT 157,NS,FDGS(NS),RSG(NS)
  157 FORMAT(4X,*NS=*,I2,5X,*FDGS(NS)=*,F12.2,5X,*RSG(NS)=*,F6.2)
      PRINT 161,(VOLUME(NB),NB=1,NBED)
  161 FORMAT(4X,*VOLUME(NB)*,5X,10F8.4)
      PRINT 165,P,DP,NBED
  165 FORMAT(4X,*P=*,F6.2,5X,*DP=*,F5.2,5X,*NBED=*,I2)
      PRINT 166,H2SPPM,TIMDAY
  166 FORMAT(4X,*H2SPPM=*,F6.1,5X,*TIMDAY=*,F7.1)
      PRINT 167,TIMINT,NTIMEL
  167 FORMAT(4X,*TIMINT=*,F7.1,5X,*NTIMEL=*,I3)
      PRINT 170
  170 FORMAT(4X,*END OF INPUT DATA*)
      DO 600 NRSGAS=1,3
      DO 10 NC=NC1,NC6
   10 FC(NC)=FDGS(NS)*PERC(NC)/100.0
      FC(NC7)=FDGS(NS)*RSG(NS)
      FTS(NS)=FDGS(NS)+FC(NC7)
      FTSR=FTS(NS)
      F=FTSR
      DO 15 NC=NC1,NC7
      Y(NC)=FC(NC)/FTSR
   15 YF(NC)=Y(NC)
C***  FEED COMPOSITION CALCULATIONS ARE OVER.
C * * * * * * * * * * * * * * * * * * * * * * * * * * * * * * * * * * * * * * * * * * * *
      DO 560 NTIME=1,NTIMEL
      PRINT 456,TIMDAY
      PRINT 5,F
    5 FORMAT(//4X,*VOLUMETRIC FEED RATE OF WET GAS=F=*,F13.2)
      PRINT 65
   65 FORMAT(///4X,*CONVERTOR INLET GAS COMPOSITION(FROM INPUT DATA)*)
      GO TO 79
   19 XF=0.0
      VI=0.0
      PRINT 445
      PRINT 455
```

```
C * * * * * * * * * * * * * * * * * * * * * * * * * * * * * * * * * * * * * * * *
C***  START OF OPTIMISATION CALCULATIONS.
C---  SINCE XP(DEGREE OF CONV.OF CO IN PRODUCT GAS)IS UNKNOWN UNTIL OPTIMISATION
C---  CALCULATIONS ARE COMPLETE. SO START WITH AN ASSUMED VALUE OF XP,CALCULATE
C---  CORRESPONDING VALUE OF XF(FOR FEED)AND COMPARE THIS WITH GIVEN XF.
C---  TRIAL AND ERROR METHOD IS REPEATED TO OBTAIN XP UNTIL
C---  CALCULATED XF=GIVEN XF.
C * * * * * * * * * * * * * * * * * * * * * * * * * * * * * * * * * * * * * * * *
C---  CASE 1--CNSTRN=0. (IN THIS CASE,CONSTRAINT OF MAX.TEMP.OF 500 DEGREE C.
C---  IS NOT APPLIED.MULTIBED REACTOR IS OPTIMISED USING RATE-MATCH CRITERIA).
C---  CASE 2--CNSTRN=1. (IN THIS CASE,CONSTRAINT OF MAX.TEMP.OF 500 DEGREE C.
C---  IS APPLIED FOR 1ST BED.SO RATE-MATCHING CRITERIA IS NOT USED FOR
C---  OPTIMISING 1ST BED OF MULTIBED REACTOR.1ST BED IS OPTIMISED USING
C---  SINGLE BED OPTIMIZATION ROUTINE).
C * * * * * * * * * * * * * * * * * * * * * * * * * * * * * * * * * * * * * * * *
      TMXLMT=500.0+273.0
      CNSTRN=0.
      XESTRT=0.9600
      DELTAX=0.0100
  410 KX=0
      NB=NBED
      XE(NB)=XESTRT-DELTAX
  415 XEN=XE(NB)
      XP=XE(NB)
      VE=VOLUME(NB)
      KX=KX+1
  250 CALL SBOPTM(XEN,TEN,P,YF,ACP,BCP,CCP,F,XP,DP,XIN,TIN,VI,VE,
     1TIMDAY,H2SPPM)
      TE(NB)=TEN
      XI(NB)=XIN
      TI(NB)=TIN
      IF(NBED-1)300,300,475
  475 IF(CNSTRN)480,260,480
  480 IF(NB-2)300,485,260
  485 XE(NB-1)=XI(NB)
      NB=NB-1
      XEN=XE(NB)
      GO TO 250
  260 CALL RATMCH(XIN,TIN,P,YF,XP,DP,RATIN,TEN1,TIMDAY,H2SPPM)
      RATI(NB)=RATIN
      TE(NB-1)=TEN1
      XE(NB-1)=XI(NB)
      NB=NB-1
      TEN=TE(NB)
      XEN=XE(NB)
      VE=VOLUME(NB)
      CALL MATENG(XEN,TEN,P,YF,ACP,BCP,CCP,F,XP,DP,XIN,TIN,VI,VE,
     1TIMDAY,H2SPPM)
      TI(NB)=TIN
      XI(NB)=XIN
```

```
      IF(NB-1)3[illegible],3[illegible],475
  300 DO 325 NB=1,NBED
      XIOPTM(NB)=XI(NB)
      XEOPTM(NB)=XE(NB)
      TIOPTM(NB)=TI(NB)
      TEOPTM(NB)=TE(NB)
  325 CONTINUE
      PRINT 345,NBED,XE(NBED)
  345 FORMAT(/5X,*ASSUMED VALUE OF DEGREE OF CONVERSION AT REACTOR EXIT
     1=XE(*,I2,*)=*,F3.5)
      PRINT 346
  346 FORMAT(/7X,*NB*,9X,*XIOPTM(NB)*,9X,*XEOPTM(NB)*,9X,*TIOPTM(NB)*,
     19X,*TEOPTM(NB)*)
      PRINT 347,(NB,XIOPTM(NB),XEOPTM(NB),TIOPTM(NB),TEOPTM(NB),
     1NB=1,NBED)
  347 FORMAT(6X,I3,2F19.4,2F19.2)
  420 XI1DIF=XIOPTM(1)-XF
      XIEROR=ABS(XI1DIF)
      IF(XIEROR-[illegible])45[illegible],425,425
  425 IF(XI1DIF)43[illegible],450,435
  430 DELTAX=DELTAX*0.250
      IF(KX-1)410,410,440
  435 NB=NBED
      XEOLD=XE(NB)
  440 NB=NBED
      XE(NB)=XEOLD-DELTAX
      GO TO 415
  450 PRINT 455
  455 FORMAT(/1X,120(1H*)/)
      DO 330 NB=1,NBED
      XEXITB=XE(NB)
      TEEQLM(NB)=TEQ(YF,XEXITB)
  330 CONTINUE
      PRINT 445
  445 FORMAT(1H1)
      PRINT 455
      PRINT 460
  460 FORMAT(/5X,2H**,*FINAL OPTIMUM CONDITIONS FOR REACTOR BEDS*,2H**/)
      PRINT 456,TIMDAY
  456 FORMAT(7X,*TIME ON STREAM(IN DAYS)=*,F7.1/)
      PRINT 220,FDGS(1)
  220 FORMAT(4X,*INLET DRY GAS FLOW=*,F12.2)
      PRINT 225,RSG(1)
  225 FORMAT(4X,*INLET STEAM/GAS RATIO=*,F6.2)
      IF(CNSTRN)510,500,510
  500 PRINT 505
  505 FORMAT(7X,*CONSTRAINT OF MAX.TEMP.OF 500DEGREE C.IS NOT APPLIED.*)
      PRINT 506
  506 FORMAT(7X,*MULTIBED REACTOR IS OPTIMISED USING RATE-MATCHING CRITE
     1RIA*/)
```

```
      GO TO 520
  510 PRINT 515
  515 FORMAT(7X,*CONSTRAINT OF MAX.TEMP.OF 500 DEGREE C. IS APPLIED FOR
     11ST BED*)
      PRINT 516
  516 FORMAT(7X,  *RATE-MATCHING CRITERIA IS NOT USED FOR OPTIMISING 1ST
     1BED*/)
  520 CONTINUE
      PRINT 348
  348 FORMAT(/6X,*BED*,11X,*INLET*,15X,*EXIT*,16X,*INLET*,
     114X,*EXIT*,16X,*EQUILIBRIUM*)
      PRINT 349
  349 FORMAT(6X,*NO.*,9X,*CONVERSION*,9X,*CONVERSION*,13X,*TEMP.*,
     114X,*TEMP.*,16X,*EXIT TEMP.*)
      PRINT 350
  350 FORMAT(/  7X,*NB*,9X,*XIOPTM(NB)*,9X,*XEOPTM(NB)*,9X,*TIOPTM(NB)*,
     19X,*TEOPTM(NB)*,9X,*TEEQLM(NB)*)
      PRINT 351,(NB,XIOPTM(NB),XEOPTM(NB),TIOPTM(NB),TEOPTM(NB),
     1TEEQLM(NB),NB=1,NBED)
  351 FORMAT(6X,I3,2F19.4,3F19.2)
C*****************************************************************************
C***  FINDING COMPOSITIONS FOR DIFFERENT BEDS
      NB=1
      NS=1
      NC1=1
      NC2=NC1+1
      NC6=NC1+5
      NC7=NC1+6
   25 X(NS)=XIOPTM(NB)
      TCS(NS)=TIOPTM(NB)-TKO
      X(NS+1)=XEOPTM(NB)
      TCS(NS+1)=TEOPTM(NB)-TKO
      XEXIT=X(NS+1)
      GO TO 100
  100 NC1=NC1+7
      NC2=NC2+7
      NC6=NC6+7
      NC7=NC7+7
      NCL1=NC1-7
  102 CALL MASS(NC1,YF,XEXIT,Y)
      YCONV(NB)=YF(2)*(X(NS+1)-X(NS))
   33 CONV(NB)=YCONV(NB)*FTSR
      DO 35 NC=NC1,NC7
   35 FC(NC)=Y(NC)*FTSR
      FDGS(NS+1)=FTSR-FC(NC7)
      DO 37 NC=NC1,NC6
   37 PERC(NC)=100.0*FC(NC)/FDGS(NS+1)
      PRINT 70,NB,CONV(NB),NS
   70 FORMAT(///4X,11HBED NO.=NB=I2,16X,20HCONVERSION=CONV(NB)=F9.2,
     15X,*STREAM NO.=NS=*,I3)
```

```
      PRINT 75,TCS(NS),TCS(NS+1),X(NS),X(NS+1)
   75 FORMAT(4X,16HTEMP.IN=TCS(NS)=F7.2,6X,20HTEMP.EXIT=TCS(NS+1)=F9.2,
     15X,*X(NS)=*,F7.4,5X,*X(NS+1)=*,F7.4)
      PRINT 95,NB,VOLUME(NB)
   95 FORMAT(/4X,*TOTAL VOLUME OF BED*,I2,*=*,F7.3)
      PRINT 96,NB
   96 FORMAT(/3X,1H*,*COMPOSITION OF GAS EXIT BED*,I2,1H*)
   79 PRINT 80
   80 FORMAT(/4X,9HCOMPONENT,9X,4HFLOW,10X,11HMOLE FRACN.,6X,13HPERCENT
     1COMP.)
      PRINT 82
   82 FORMAT(7X,2HNC,11X,6HFC(NC),11X,6H Y(NC),11X,8HPERC(NC)/)
   84 PRINT 85,(NC,FC(NC), Y(NC),PERC(NC),NC=NC1,NC6)
   85 FORMAT(6X,I3,10X,F9.2,9X,F7.4,12X,F6.2)
      NC=NC7
      PRINT 88,NC,FC(NC),Y(NC)
   88 FORMAT(6X,I3,7X,F12.2,9X,F7.4)
   89 IF(NC1-1)19,19,90
   90 IF(NB-NBED)92,60,60
   92 NB=NB+1
      NS=NS+2
      GO TO 25
   60 CONTINUE
      PRINT 455
      IF(TEOPTM(1)-TMXUMT)550,550,525
  525 CNSTRN=1.
      XESTRT=XEOPTM(NBED)+0.0150
      DELTAX=0.0025
      PRINT 445
      PRINT 455
      GO TO 410
  550 CONTINUE
      PRINT 445
      NB=1
      NS=1
      NC1=1
      NC2=NC1+1
      NC6=NC1+5
      NC7=NC1+6
      TIMDAY=TIMDAY+TIMINT
  560 CONTINUE
      IF(NRSGAS-2)625,650,600
  625 RSG(NS)=1.50
      FDGS(NS)=22500.00
      GO TO 600
  650 RSG(NS)=1.50
      FDGS(NS)=13500.00
  600 CONTINUE
      STOP
      END
```

```
      SUBROUTINE SBOPTM(XE,TEOPTM,P,YF,ACP,BCP,CCP,F,XP,DP,XIOPTM,
     1TIOPTM,VI,VE,TIMDAY,H2SPPM)
C---  THE PURPOSE OF SUBROUTINE SBOPTM IS TO OPTIMISE A SINGLE BED OF THE
C---  REACTOR.VALUE OF BED VOLUME AND XE(DEGREE OF CONV.OF CO AT BED EXIT)
C---  IS GIVEN.THIS SUBROUTINE FINDS TEOPTM(OPTM.EXIT BED TEMP.),
C---  TIOPTM(OPTM.INLET TEMP),XIOPTM(OPTM.INLET DEGREE OF CONV.OF CO)
C---  TO GET MAX.CONVERSION IN THE BED.
C---  TEMP. T IS IN DEGREE K.
C***  MAXIMIZATION USING MODIFIED FIBONACCI SEARCH
      DIMENSION ACP( 7),BCP( 7),CCP( 7),YF(10)
      TEQE=TEQ(YF,XE)
      TMXLMT=500.0+273.0
      K=1
      TELOW=325.0+273.0
      IF(TMXLMT-TEQE)5,6,6
    5 TEHIGH=TMXLMT
      GO TO 7
    6 TEHIGH=TEQE
    7 CONTINUE
   10 TERANG=TEHIGH-TELOW
      TELOCT=0.3820*TERANG
      TE1=TELOW+TELOCT
C***  AS WE ARE PROCEEDING FROM LAST STAGE TO FIRST STAGE,EXIT CONDITIONS OF
C***  REACTOR IN THIS ARGUMENT LIST CORRESPOND TO INLET CONDNS.IN THE
C***  ARGUMENT LIST OF SUBROUTINE MATENG.
      CALL MATENG(XE,TE1,P,YF,ACP,BCP,CCP,F,XP,DP,XI1,TI1,VI,VE,
     1TIMDAY,H2SPPM)
      XCONV1=XE-XI1
      TE2=TEHIGH-TELOCT
      CALL MATENG(XE,TE2,P,YF,ACP,BCP,CCP,F,XP,DP,XI2,TI2,VI,VE,
     1TIMDAY,H2SPPM)
      XCONV2=XE-XI2
   20 TEDIFF=TE2-TE1
      TEEROR=ABS(TEDIFF)/TE1
      IF (TEERROR-0.001)70,30,30
   30 IF (XCONV1-XCONV2)50,60,40
   40 K=K+1
      TELOW=TELOW
      TEHIGH=TE2
      TERANG=TEHIGH-TELOW
      TELOCT=0.3820*TERANG
      TE2=TE1
      TI2=TI1
      XI2=XI1
      XCONV2=XCONV1
      TE1=TELOW+TELOCT
      CALL MATENG(XE,TE1,P,YF,ACP,BCP,CCP,F,XP,DP,XI1,TI1,VI,VE,
     1TIMDAY,H2SPPM)
      XCONV1=XE-XI1
      GO TO 20
```

```
   50 K=K+1
      TELOW=TE1
      TEHIGH=TEHIGH
      TERANG=TEHIGH-TELOW
      TELOCT=0.3820*TERANG
      TE1=TE2
      TI1=TI2
      XI1=XI2
      XCONV1=XCONV2
      TE2=TEHIGH-TELOCT
      CALL MATENG(XE,TE2,P,YF,ACP,BCP,CCP,F,XP,DP,XI2,TI2,VI,VE,
     1TIMDAY,H2SPPM)
      XCONV2=XE-XI2
      GO TO 20
   60 K=K+1
      TELOW=TE1
      TEHIGH=TE2
      GO TO 10
   70 IF(XCONV1-XCONV2)90,90,80
   80 XCOPTM=XCONV1
      TEOPTM=TE1
      TIOPTM=TI1
      XIOPTM=XI1
      GO TO 100
   90 XCOPTM=XCONV2
      TEOPTM=TE2
      TIOPTM=TI2
      XIOPTM=XI2
      GO TO 100
  100 CONTINUE
  160 RETURN
      END
      SUBROUTINE RATMCH(XIN,TIN,P,YF,XP,DP,RATIN,TEN1,TIMDAY,H2SPPM)
C---   RATE-MATCHING PROGRAM SATISFIES FOLLOWING CONDITIONS BETWEEN TWO
C---   BEDS (N-1)AND N.
C---   CONDN.1  RATE AT EXIT OF BED(N-1)=RATE AT INLET TO BED N.
C---   CONDN.2  XE AT EXIT OF BED (N-1)=XI AT INLET TO BED N.
C---   CONDN.3  TEMP.AT EXIT OF BED (N-1) IS GREATER THAN TEMP.AT INLET TO BED
      DIMENSION YF(10)
      XMEAN=XIN
      CALL RATEQN(XIN,TIN,P,YF,XP,DP,XEQLIN,RATIN,XMEAN,TIMDAY,H2SPPM)
C---   N1=NL=BED(N-1)
C---   N2=BED N
      XENL=XIN
      DELTAT=20.0
   10 K=0
      TENL=TIN+DELTAT
   15 K=K+1
      CALL RATEQN(XENL,TENL,P,YF,XP,DP,XEQLNL,RATENL,
     1XMEAN,TIMDAY,H2SRPM)
```

```
    20 RATDIF=RATENL-RATIN
       RTEROR=ABS(RATDIF)/RATIN
       IF(RTEROR-0.001)50,25,25
    25 IF (RATDIF)30,50,35
    30 DELTAT=DELTAT*0.250
       IF(K-1)10,10,40
    35 TEOLD=TENL
    40 TENL=TEOLD+DELTAT
       GO TO 15
C***   FOLLOWING CONDNS.CORRESPOND TO EQUAL RATES AT EXIT OF BED N1
C***   AND ENTRANCE OF BED N2.
    50 RATIN2=RATIN
       RATEN1=RATENL
       XEN1=XENL
       TEN1=TENL
       RETURN
       END
       FUNCTION TEQ(YF,X)
C---   THIS FN.FINDS TEQ(EQUIL.TEMP.) IN DEGREE K AT A GIVEN  DEGREE OF
C---   CONVERSION X AND FEED COMPOSITION YF(MOLE FRACN.)
       DIMENSION YF(10)
       XEQUIL=X
       YCONV=YF(2)*XEQUIL
       EQUILK=((YF(3)+YCONV)*(YF(1)+YCONV))/((YF(2)-YCONV)*(YF(7)-YCONV))
C---   FINDING TEMP.CORRESPONDING TO EQUILK(ACTUAL VALUE OF EQUIL.CONST.)
C---   BY TRIAL AND ERROR SEARCH.
       TMAX=900.0+273.0
       DELTAT=200.0
    10 KI=0
       TEQGES=TMAX-DELTAT
    15 KI=KI+1
       EQKGES=EQK(TEQGES)
C---   EQKGES IS VALUE OF EQUIL.CONST.AT A GUESSED TEMP. TEQGES.
    20 EQKDIF=EQKGES-EQUILK
       EKEROR=ABS(EQKDIF)/EQUILK
       IF (EKEROR-0.001)50,25,25
    25 IF (EQKDIF)35,50,30
    30 DELTAT=DELTAT*0.250
       IF (KI-1)10,10,40
    35 TEQOLD=TEQGES
    40 TEQGES=TEQOLD-DELTAT
       GO TO 15
    50 TEQ=TEQGES
       RETURN
       END
       SUBROUTINE MATENG(XI,TI,P,YF,A,B,C,F,XP,DP,XE,TE,VE,VI,
      1TIMDAY,H2SPPM)
C***   SIMULATION OF SHIFT REACTOR(FINDING CONV.AND TEMP.FROM GIVEN VOLUME)
C      PERFORMS MATERIAL-ENERGY BALANCE.V IS INDEPENDENT VARIABLE.
C      THIS SUBROUTINE SOLVES TWO SIMULTANEOUS FIRST-ORDER DIFFERENTIAL
```

```
C       EQNS. USING RUNGE-KUTTA METHOD. FINDS X(DEGREE OF CONV. OF CO)
C       AND T(TEMP.) AS A FN.OF V(CATALYST VOL.) BETWEEN VI=0 AND VE=VOLUME(NB)
C       INITIAL CONDITIONS VI,XI,TI ARE GIVEN.
        DIMENSION A( 7),B( 7),C( 7),YF(10)
        DIMENSION X(100),T(100),V(100)
        DIMENSION XEQL(100),RATE(100),TTRY(100)
        K=0
        NINTVL=5
   35   K=K+1
        NINTVL=NINTVL+5
   10   DELTAV=(VE-VI)/FLOAT(NINTVL)
        JNO=0+1
        JNINT=NINTVL+1
        X(JNO)=XI
        T(JNO)=TI
        V(JNO)=VI
        DO 20 JN=JNO,JNINT
        XMEAN=X(JN)
        N=JN-1
        XJN1=X(JN)
        TJN1=T(JN)
        CALL RATEQN(XJN1,TJN1,P,YF,XP,DP,XEQJN1,RATJN1,
       1XMEAN,TIMDAY,H2SRPM)
        AL1=DELTAV*DTBYDX(XJN1,TJN1,P,YF,A,B,C)*DXBYDV(RATJN1,F,YF)
        AK1=DELTAV*DXBYDV(RATJN1,F,YF)
        XEQL(JN)=XEQJN1
        RATE(JN)=RATJN1
        XJN2=X(JN)+AK1/2.0
        TJN2=T(JN)+AL1/2.0
        CALL RATEQN(XJN2,TJN2,P,YF,XP,DP,XEQJN2,RATJN2,
       1XMEAN,TIMDAY,H2SRPM)
        AL2=DELTAV*DTBYDX(XJN2,TJN2,P,YF,A,B,C)*DXBYDV(RATJN2,F,YF)
        AK2=DELTAV*DXBYDV(RATJN2,F,YF)
        XJN3=X(JN)+AK2/2.0
        TJN3=T(JN)+AL2/2.0
        CALL RATEQN(XJN3,TJN3,P,YF,XP,DP,XEQJN3,RATJN3,
       1XMEAN,TIMDAY,H2SRPM)
        AL3=DELTAV*DTBYDX(XJN3,TJN3,P,YF,A,B,C)*DXBYDV(RATJN3,F,YF)
        AK3=DELTAV*DXBYDV(RATJN3,F,YF)
        XJN4=X(JN)+AK3
        TJN4=T(JN)+AL3
        CALL RATEQN(XJN4,TJN4,P,YF,XP,DP,XEQJN4,RATJN4,
       1XMEAN,TIMDAY,H2SRPM)
        AL4=DELTAV*DTBYDX(XJN4,TJN4,P,YF,A,B,C)*DXBYDV(RATJN4,F,YF)
        AK4=DELTAV*DXBYDV(RATJN4,F,YF)
        DELTAX=(AK1+2.0*AK2+2.0*AK3+AK4)/6.0
        DELTAT=(AL1+2.0*AL2+2.0*AL3+AL4)/6.0
        T(JN+1)=T(JN)+DELTAT
        V(JN+1)=V(JN)+DELTAV
        X(JN+1)=X(JN)+DELTAX
```

```
   20 CONTINUE
      TTRY(K)=T(JNINT)
      IF(K-1)35,35,40
   40 ERROR=ABS(TTRY(K)-TTRY(K-1))
      IF((ERROR/TTRY(K))-.001)50,35,35
   50 TE=TTRY(K)
      XE=X(JNINT)
      XEQLE=XEQL(JNINT)
      RATEE=RATE(JNINT)
      XEQLI=XEQL(JNO)
      RATEI=RATE(JNO)
      RKPRNT=1.0
      IF(RKPRNT)90,55,90
   55 PRINT 60
   60 FORMAT(///5X,*RUNGE-KUTTA INTEGRATION*)
      PRINT 75,XI,XEQLI,TI,VI,RATEI
   75 FORMAT(5X,*XI=*,F7.4,5X,*XEQLI=*,F7.4,5X,*TI=*,F7.2,5X,
     1*VI=*,F7.3,5X,*RATEI=*,E15.3/)
      PRINT 80,XE,XEQLE,TE,VE,RATEE
   80 FORMAT(5X,*XE=*,F7.4,5X,*XEQLE=*,F7.4,5X,*TE=*,
     1F7.2,5X,*VE=*,F7.3,5X,*RATEE=*,E15.3///)
   90 CONTINUE
      RETURN
      END
      FUNCTION DTBYDX(X,T,P,YF,A,B,C)
      DIMENSION YF(10),A( 7),B( 7),C( 7),Y(100),CPO(10)
      DATA U,V,W,AK1,AK2,TO,AD,BD,CD/0.63E14,-5.56,1.29,0.933E04,
     1-0.93539E-03,600.0,-0.201,5.493E-03,-2.7177E-06/
      CALL MASS(1,YF,X,Y)
      CPOSUM=0.0
      DO 10 I=1,7
      CPO(I)=A(I)+B(I)*T+C(I)*(T**2.0)
      CPOSUM=CPOSUM+Y(I)*CPO(I)
   10 CONTINUE
      CPRSUM=CPOSUM+Y(7)*U*(P**W)*(T**V)
      HRTOP=-AK1*EXP(AK2*P)
      C1=((AD*TO)+(BD*(TO**2.0))/2.0+(CD*(TO**3.0))/3.0)
      C2=U/(V+1.0)
      C3=(U/(V+1.0))*(TO**(V+1.0))
      HRTP=HRTOP+((AD*T)+(BD*(T**2.0)/2.0)+(CD*(T**3.0)/3.0)
     1-(C2*(P**W)*(T**(V+1.0))))+C3*(P**W)-C1
      DTBYDX=(-HRTP*YF(2))/CPRSUM
      RETURN
      END
      FUNCTION DXBYDV(RATE,F,YF)
C     DXBYDV=DX/DV
      DIMENSION YF(10)
      DXBYDV=RATE/(F*YF(2))
      RETURN
      END
```

```
      SUBROUTINE RATEQN(X,T,P,YF,XP,DP,XEQL,RATE,XMEAN,TIMDAY,H2SPPM)
C***  RATEQN CALCULATES PSEUDO FIRST-ORDER REACTION RATE OBTAIN5D
C***  BY SIMPLIFYING SECOND ORDER RATE EXPRESSION(LAUPICHLER,MOE).
C***  BASED ON RUTHVENS METHOD FOR FCI HT SHIFT CATALYST
C***  RATE EQN IS DEVELOPED FOR PRESSURE RANGE 6-26 KG/SQ.CM.ABS
C***  UNITS-- TIMDAY=TIME IN DAYS(ON STREAM)---(GREATER THAN 1 DAY)
C***  UNITS-- H2SPPM=CONCN.OF H2S IN PPM.(DRY BASIS)
C***  UNITS-- TEMPERATURE=T DEGREE K.
C***  UNITS-- PRESSURE=P KG/SQ.CM.ABS
C***  DP=EFFECTIVE PARTICLE DIA IN CM. =6*VP/AP
C***  RK STANDS FOR RATE CONST. K
C * *  * * * * * * * * * * * * * * * * * * * * * * * * * * * * * * * * * * * *
      DIMENSION YF(10),YMEAN(10)
C---  ZCORCN=CORRECTION FACTOR FOR RATE CONSTANT.
      ZCORCN=1.0
      R=1.987
      ZO=4.22E03
      ZTIME=TIMDAY**(-0.079)
      IF (H2SPPM-2.7)15,16,16
   15 ZSULFR=1.0
      GO TO 20
   16 ZSULFR=((-0.276)*ALOG10(H2SPPM))+1.127
   20 CONTINUE
      FA=13.430
      ZPRESS=(EXP(-FA/P))/P
      EA=(9.225E03)*R
      ZTEMP=EXP(-EA/(R*T))
      RKV=ZO*ZTIME*ZPRESS*ZTEMP*ZSULFR*ZCORCN
      DIFFP1=0.043
      DIFF=(DIFFP1/P)*((T/673.0)**1.5)
      THMOD=(DP/2.0)*SQRT(RKV/DIFF)
      IF (THMOD)35,25,35
   25 EFF=1.0
      GO TO 40
   35 CONTINUE
      EFF=(3.0/THMOD)*((1.0/TANH(THMOD))-(1.0/THMOD))
   40 CONTINUE
      VOID=0.4
      RKO=RKV*EFF*(1.0-VOID)
      RKA=273.0*3600.0*(P/T)*RKO
      YMEAN(7)=YF(7)-YF(2)*XMEAN
      RATE=(RKA*YF(2))*(XEQ(YF,T)-X)*YMEAN(7)
      XEQL=XEQ(YF,T)
      RETURN
      END
      FUNCTION XEQ(YF,T)
C     THIS FN. CALCULATES XEQ(DEGREE OF CONVERSION OF CO) AT A GIVEN
C     TEMP. T DEGREE K AND FEED COMPOSITION YF(MOLE FRACN.)
      DIMENSION YF(10)
      A1=EQK(T)-1.0
```

```
      B1=(-EQK(T)*YF(2))-(EQK(T)*YF(7))-YF(3)-YF(1)
      C1=(EQK(T)*YF(2)*YF(7))-(YF(3)*YF(1))
      YCONV2=(-B1-SQRT((B1*B1)-(4.0*A1*C1)))/(2.0*A1)
      YCOEQ2=YF(2)-YCONV2
      IF(YCOEQ2)50,25,25
   25 YCOEQ=YCOEQ2
      GO TO 30
   50 YCONV1=(-B1+SQRT((B1*B1)-(4.0*A1*C1)))/(2.0*A1)
      YCOEQ1=YF(2)-YCONV1
      IF(YCOEQ1)70,20,20
   20 YCOEQ=YCOEQ1
   30 XEQ=(YF(2)-YCOEQ)/YF(2)
      XEQL=XEQ
      EQUILK=EQK(T)
      GO TO 80
   70 PRINT 75,YCOEQ1,YCOEQ2
   75 FORMAT(5X,*YCOEQ1=*,F7.4,5X,*YCOEQ2=*,F7.4,5X,
     1*THIS IS NOT POSSIBLE*)
   80 RETURN
      END
      FUNCTION EQK(T)
C     THIS FN. CALCULATES EQUILIBRIUM CONSTANT EQK FOR WATER GAS SHIFT
C     REACTION AT A GIVEN TEMPERATURE T DEGREE K.
      DATA R,AD,BD,CD,HDO,CONS1,SDO,CONS2/1.987,-0.201,5.493E-03,
     1-2.7177E-06,-9838.0,160.220,-10.042,0.372/
      HDT=HDO+((AD*T)+(BD*T*T/2.0)+(CD*(T**3.0)/3.0))-CONS1
      SDT=SDO+((AD*ALOG(T))+(BD*T)+(CD*T*T/2.0))-CONS2
      FDT=HDT-(T*SDT)
      EQK=EXP(-FDT/(R*T))
      RETURN
      END
      SUBROUTINE MASS(NC1,YF,XT,Y)
C***  STOICHIOMETRIC RELATIONS
      DIMENSION YF(10),Y(10)
      YCONVT=YF(2)*XT
      Y(NC1)=YF(1)+YCONVT
      Y(NC1+1)=YF(2)-YCONVT
      Y(NC1+2)=YF(3)+YCONVT
      Y(NC1+3)=YF(4)
      Y(NC1+4)=YF(5)
      Y(NC1+5)=YF(6)
      Y(NC1+6)=YF(7)-YCONVT
      RETURN
      END
      29.00          0.60              3
      53.20         40.60           3.20          0.40          2.60          0.80
   31500.00          2.00
      4.350         8.700          8.700
       45.0         270.0
        60              1
```

REFERENCES

1. Denbigh, K.G. and Turner, J.C.R.; "Chemical Reactor Theory" Cambridge University Press, (1971).
2. Horn, F. and Kuchler, L.; Chem.Ing. Techn. 31, 1(1959).
3. Bilous, O. and Amundson, N.R.; Chem. Engng. Sci., 5, 81, 115 (1956).
4. Kramer, H. and Westerterp, K.R.; "Elements of Chemical Reactor Design and Operation" Netherlands University Press, Amsterdam (1963).
5. Laupichler, F.G.; Ind. Eng. Chem., 30, 578 (1938).
6. Padovani, C. and Lotteri, A.; J. Soc. Chem. Ind., 56, 391 T(1937).
7. Kulkova, N.V. and Temkin, M.I., Zhur. Fiz. Khim. 23, 695 (1949); Chem. Abstrs., 43, 7308h (1949).
8. Atwood, K., Arnold, M.R. and Appel, E.G., Ind. Eng. Chem. , 42, 1600 (1950).
9. Mars, P., Chem. Engng. Sci., 14, 375 (1961).
10. Popov, B.I., Zhur. Fiz. Khim., 31, 1033 (1951).
11. Barkley, L.W., Corrigan, T.E., Wainwright, H.W. and Sands, A.E., Ind. Eng. Chem., 44, 1066 (1952).
12. Kodama, S., Fukui, K., Tame, T.; and Kinoshita, M., Catalysts (Japan), 8, 50 (1952).
13. Kodama, S., Mazume, A., Fukuba, K. and Fukui, K., Bull. Chem. Soc. Japan, 28, 318 (1955).
14. Bortolini, P., Chem. Engng. Sci., 9, 135 (1958).
15. Stelling, O., and Krusenstierna, O. Von, Acta Chem. Scand., 12, 1095 (1958).

16. Kirrillov, I.P., Trudy Ivanovsk. Khim.-Tekhnol. Inst., No.5, 45 (1956); Chem. Abstr. 53, 11969 (1959).
17. Atroshchenko, V.I., and Bibr. B., Zhur. Priklad. Khim., 32, 997 (1959); Chem. Abstr. 53, 15735 (1959).
18. Hulburt, H.M., and Vasan, C.D.S., A.I.Ch.E. Journal, 7, 143 (1961).
19. Bohlbro, H., Acta Chem. Scand., 15, 502 (1961).
20. Atroshchenko, V.I., Zhidkov, B.A. and Zasorin, A.P., Kinetika i Kataliz, 3, 605 (1962). English Translation in Kinetics and Catalysis, 3 529 (1962).
21. Goodridge, F., and Quazi, H.A., Trans. Inst. Chem. Engrs., 45, T274 (1967).
22. Moe, J.M., Chem.Eng. Progr., 58, No.3,33 (1962).
23. Hougen, O.A., Watson, K.M., and Ragatz, R.A., "Chemical Process Principles", Part I, John Wiley & Sons, Inc. (1954).
24. Hilsenrath, J., Beckett, C.W., Benedict, W.S., Fano, L., Hoge, H.J., Masi, J.F., Nuttall, R.L., Toulokian, Y.S., and Wolley, H.W., "Tables of Thermodynamic & Transport Properties" Pergamon Press, Oxford (1960).
25. Ruthven, D.M., Chem. Eng. Sci. 23, 759 (1968).
26. Ruthven, D.M., Cand. J. Chem. Eng., 47, 327 (1969).
27. Thiele, E.W., Ind. Eng. Chem., 31, 916 (1939).
28. Hoogschagen, J., Ind. Eng. Chem., 47, 906 (1955).
29. Satterfield, C.N. and Sherwood, T.K., "The Role of Diffusion in Catalysis", Addison-Wesley (1963).

30. Chandra, M., Singh, S.S., Banerjee, B., Sinha, A.K. and Sinha, N.K., Paper presented at "The 24th Annual General Meeting of Indian Institute of Chemical Engineers" held at IIT-Kanpur (Feb. 1972).

31. Mahapatra, H., Ray, N., Sen, B. and Sen, S.P., Technology, 8, 211 (1971).

32. Ting, A.P. and Wan, S.W., Chem. Engg., May 19, 185 (1969).

33. Banerjee, B., Chandra, M. and Ghosal, S.R., Paper presented at "The 24th Annual General Meeting of Indian Institute of Chemical Engineers" held at IIT-Kanpur (Feb. 1972).

34. Lavrov, N.V., Korobov, V.V. and Filippova, V.I., "The Thermodynamics of Gasification and Gas-Synthesis Reactions", Pergamon Press (1963).

35. Smith, J.M., "Chemical Engineering Kinetics", McGraw-Hill Book Company (1956).

36. Laupidus, L., "Digital Computation for Chemical Engineers" McGraw-Hill, New York (1962).

37. Aris, R., "Optimal Design of Chemical Reactors", Academic Press, New York (1961).

38. Horn, V.F., Z. Elektrochem., 65, 295 (1961).

39. Rafal, M.D., and Dranoff, J.S., Ind. Eng. Chem., Process Design Develop., 5, 129 (1966).

40. Beveridge, G.S. and Schechter, R.S., "Optimization: Theory and Practice" McGraw-Hill, New York (1970).